YAŞAR UNIVERSITY
GRADUATE SCHOOL

MASTER THESIS

ANALYSIS OF ALBEDO EFFECT IN A 30-KW BIFACIAL PV SYSTEM WITH DIFFERENT GROUND SURFACES USING PVSYST SOFTWARE

ERSAGUN TÜRKDOĞRU

THESIS ADVISOR: ASSIST. PROF.(PhD) MAHİR KUTAY

DEPARTMENT OF ELECTRICAL AND ELECTRONICS ENGINEERING

PRESENTATION DATE: 28.06.2022

BORNOVA / İZMİR
JUNE 2022

We certify that, as the jury, we have read this thesis and that in our opinion it is fully adequate, in scope and in quality, as a thesis for the degree of Master of Science /Master of Arts/ the Doctor of Philosophy/Proficiency in Art.

Jury Members:	**Signature:**
Assist./Assoc./Prof.(PhD) Xxx YYY … University	.....
Assist./Assoc./Prof.(PhD) Xxx YYY … University	.....
Assist./Assoc./Prof.(PhD) Xxx YYY … University	.....
Assist./Assoc./Prof.(PhD) Xxx YYY … University	.....
Assist./Assoc./Prof.(PhD) Xxx YYY … University	.....
Assist./Assoc./Prof.(PhD) Xxx YYY … University	.....

Prof. (PhD) Yucel Ozturkoglu

Director of the Graduate School

ABSTRACT

ANALYSIS OF ALBEDO EFFECT IN A 30-KW BIFACIAL PV SYSTEM WITH DIFFERENT GROUND SURFACES USING PVSYST SOFTWARE

TÜRKDOĞRU, Ersagun

MSc., Electrical and Electronics Engineering

Advisor: Assist. Prof. (PhD) Mahir KUTAY

June 2022

Today, electrical energy is used extensively worldwide, increasing importance in almost all business sectors. For this reason, how to produce electrical power from earth sources is so important. Renewable energy sources that do not damage the environment and do not cause greenhouse gas emissions are increasingly used in electrical energy production. Solar energy, also renewable energy, is an excellent choice for the world's future because it is durable, abundant, low cost, recycling, and clean. Efficiency in solar energy is essential in terms of reducing resource use. Solar PV modules' efficiency depends on their structure, irradiance, and temperature. The albedo effect is directly effective in the bifacial modules because of the surface reflection of direct and diffuse irradiances. This master thesis aims to analyze the contribution of the Albedo effect, which is the reflective power of the surface, to the gain and efficiency in a 30-kW bifacial PV system doing simulations with PVsyst software. This PV system was simulated under different ground models and albedo values in the PVsyst software. After the results were analyzed, it was realized that the albedo effect gives a serious power increase in bifacial PV systems compared to mono facial PV systems.

keywords: Albedo Effect, PV System Efficiency, Bifacial Modules, PVsyst Software, Lowering LCOE

ÖZ

ALBEDO ETKİSİNİN FARKLI YER ZEMİNLERİ ILE 30 KW ÇİFT YÜZLÜ PV SİSTEMİNDE PVSYST YAZILIMI KULLANILARAK ANALİZ EDİLMESİ

TÜRKDOĞRU, Ersagun
Yüksek Lisans Tezi, Elektrik – Elektronik Mühendisliği
Danışman: Dr.Öğr.Üyesi Mahir KUTAY
Haziran 2022

Günümüzde elektrik enerjisi dünya çapında yaygın olarak kullanılmaktadır ve hemen hemen tüm iş sektörlerinde önemide giderek artmaktadır. Bu nedenle yeryüzü kaynaklarından elektrik enerjisinin nasıl üretileceği çok önemlidir. Çevreye zarar vermeyen ve sera gazı salınımına neden olmayan yenilenebilir enerji kaynakları, elektrik enerjisi üretiminde giderek daha fazla kullanılmaktadır. Aynı zamanda yenilenebilir bir enerji olan güneş enerjisi; uzun ömürlü, düşük maliyetli, geri dönüşümlü ve temiz olduğu için dünyanın geleceği için mükemmel bir seçimdir. Güneş enerjisinde de verimlilik, kaynak kullanımının azaltılması açısından son derece önemlidir. Solar PV modüllerinin verimliliği, yapılarına, aldığı ışımaya ve panel sıcaklığına bağlıdır. Albedo etkisi; direkt ve difüzyon ışınımlarının yüzeyden yansımasına bağlı olarak çift yüzlü modüllerde doğrudan etkilidir Bu yüksek lisans tezinin amacı, yüzeyin yansıtma gücü olan Albedo etkisinin 30 kW'lık çift yüzlü bir PV sisteminde kazanç ve verimliliğe katkısını, PVsyst yazılımı ile simülasyonlar yaparak analiz etmektir. Bu PV sistemi, PVsyst yazılımında farklı zemin modelleri ve albedo değerleri altında simüle edilmiştir. Sonuçlar analiz edildikten sonra albedo etkisinin, çift yüzlü PV sistemlerde tek yüzlü PV sistemlere göre ciddi bir güç artışı sağladığı görülmüştür.

Anahtar Kelimeler: Albedo Etkisi, PV Sistem Verimliliği, Çift Yüzlü Modüller, PVsyst Yazılımı, Seviyelendirilmiş Enerji Maliyeti'ni Düşürmek

ACKNOWLEDGEMENTS

Above all, I would like to state my thankfulness to my supervisor Assist. Prof. (PhD) Mahir KUTAY for his support and understanding while carrying out this study.

I would like to express my enduring love to my parents, who are always supportive, loving and caring to me in every possible way in my life.

Ersagun TÜRKDOĞRU

İzmir, 2022

TEXT OF OATH

I declare and honestly confirm that my study, titled "ANALYSIS OF ALBEDO EFFECT IN A 30-KW BIFACIAL PV SYSTEM WITH DIFFERENT GROUND SURFACES USING PVSYST SOFTWARE" and presented as a Master's Thesis, has been written without applying to any assistance inconsistent with scientific ethics and traditions. I declare, to the best of my knowledge and belief, that all content and ideas drawn directly or indirectly from external sources are indicated in the text and listed in the list of references.

Ersagun Türkdoğru

04.07.2022

TABLE OF CONTENTS

LIST OF FIGURES

LIST OF TABLES

SYMBOLS AND ABBREVIATIONS

ABBREVIATIONS:

LCOE	Levelized Cost of Energy
DiffHorr	Horizontal Diffuse Irradiation
Earray	Effective Energy at the Output of the Array
E_Grid	Energy Injected into Grid
GCR	Ground-Coverage Ratio
GlobEff	Effective Global, corr. for IAM and Shadings
GlobHor	Global Horizontal Irradiation
GlobInc	Global Incident in Collector Plane
MPPT	Maximum Power Point Tracking
PERC	Passivated Emitter and Rear Contact
Pitch	Distance Between Rows of Modules
Pnom Ratio	Installed Power (DC)/Output Power (AC)
PR	Performance Ratio
PV	Photovoltaic
STC	Standard Test Conditions
T_Amb	Ambient Temperature
Voc	Voltage at Open Circuit

SYMBOLS:

yf	Normalized System Production
yr	Reference Incident Energy in Collector Plane
Isc	Current at Short Circuit
Lc	Normalized Collection Losses
Ls	Normalized System Losses

CHAPTER 1
INTRODUCTION

Albedo is the portion of incoming radiance reflected by a surface. **Albedo takes part in a crucial part in the energy stability of the world's surface because it determines the ratio at which solar radiation is absorbed.** Albedo is formulated just when the proportion of the radiation reflected from the surface to the incoming radiation. Many PV simulation systems only provide the option for a changeless albedo - or occasionally make a different solution for the snow-covered periods. Commonly, this is a sensible estimation for traditional low-angle tilted PV systems simulation. The albedo value extends from 0 to 1. A black surface, or an academic environment that absorbs 100% of incident radiation, has a zero value. Dark-colored, rigid soil surfaces are represented by 0.1–0.2, whereas soft, light-colored soil surfaces are represented by 0.4–0.5. Snow, particularly new, thick snow, has an albedo of up to 0.9. The number 1 denotes a perfect reflector surface (a white, absolute surface) that reflects all incident energy. Albedo can be determined with Eq.(1) general formula and seen in Figure 1.1.

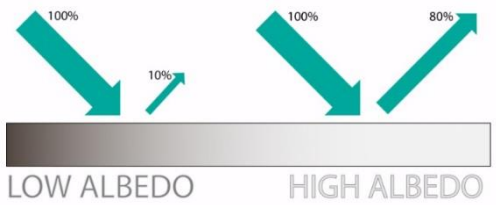

Figure 1.1. Low reflection on dark surfaces (Low Albedo) and high reflection on light surfaces (High Albedo) (From essearth.com)

$$\text{Albedo} = \frac{Reflected\ Light}{Incident\ Light} \tag{1.1}$$

The albedo, or ground reflectance, of a surface, is a unitless number that specifies how much of the incident sunlight it reflects. In most PV system demands, assuming a

changeless albedo is acceptable, but in other circumstances, a more exact description of the albedo is greatly significant. Simulation of the gain of the tilted bifacial PV modules is one instance because the energy produced on the backside will primarily originate from reflected irradiance. Albedo on the bifacial gain ranges from 5 to 15% for an albedo range of 0.2 to 0.4, according to bifacial PV module simulations of a large-scale plant. The straight, diffuse, and surface-reflected radiation of bifacial PV panel arrays are seen in Figure 1.2.

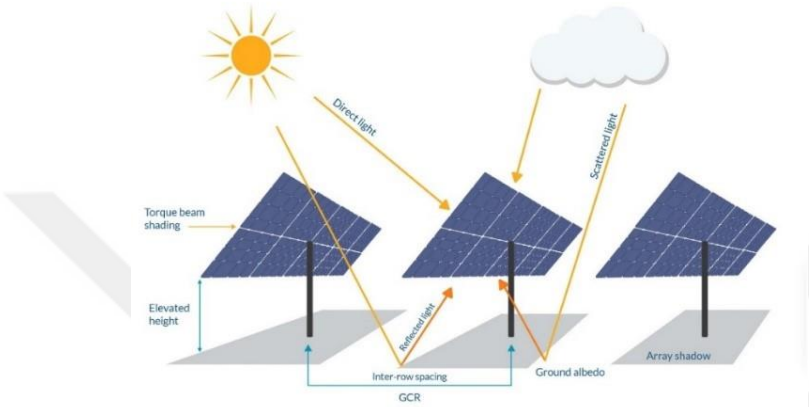

Figure 1.2. Critical factors that influence bifacial efficiency (From PVDesign)

As a result of processing the light reflected from the front and the light emitted from the rear, Both the front and rear of the bifacial PV Module may generate electricity, unlike conventional modules. Due to its capacity to gather light reflected upon the backsheet, the bifacial PV module produces more power than typical monofacial PV modules. On the back of the bifacial PV Module, instead of a white backsheet, a transparent backsheet (or glass) is used. The reflected light might come from variety places, such as the earth's surface or a nearby row of PV modules. The bifacial gain is tightly linked to the direct sunshine, diffuse light, and reflected light gained by the rear side in terms of irradiance received by the module. These computations are additionally influenced by albedo, ground covering, and mounting features. Furthermore, the bifacial gain is influenced by module quality as well as other elements like as albedo, height to the ground, ground cover ratio, and potential in different global areas. The ratio of supplemental rear side energy output (kWh) to front side energy output (kWh) determines bifacial gain (kWh). Eq.(2). Typical and bifacial solar cell structures are seen in Figure 1.3.

$$\text{Bifacial Gain (BG)} = \frac{\text{Energy (Rear)}}{\text{Energy (Front)}} \tag{1.2}$$

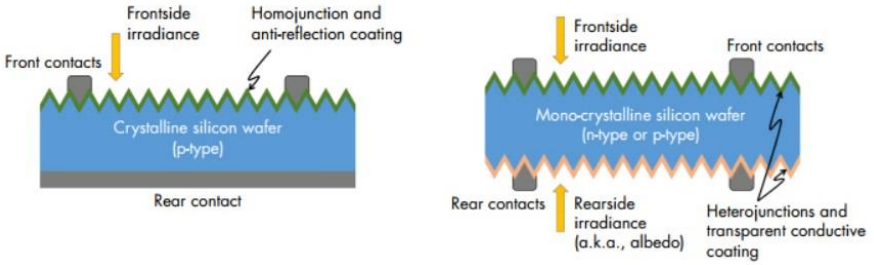

Figure 1.3. The contrast between the typical and bifacial solar cell (From EPRI)

The most rational choice is to use renewable energy sources rather than fossil fuels which are harmful to the environment. Labor loss and costs will be reduced through the most efficient use of these renewable energy resources. We can not keep using fossil fuels forever. Making recycling processes operate, decreasing resource waste, and introducing new technology will make the planet more livable. Figure 1.4 shows the albedo values of several surface materials.

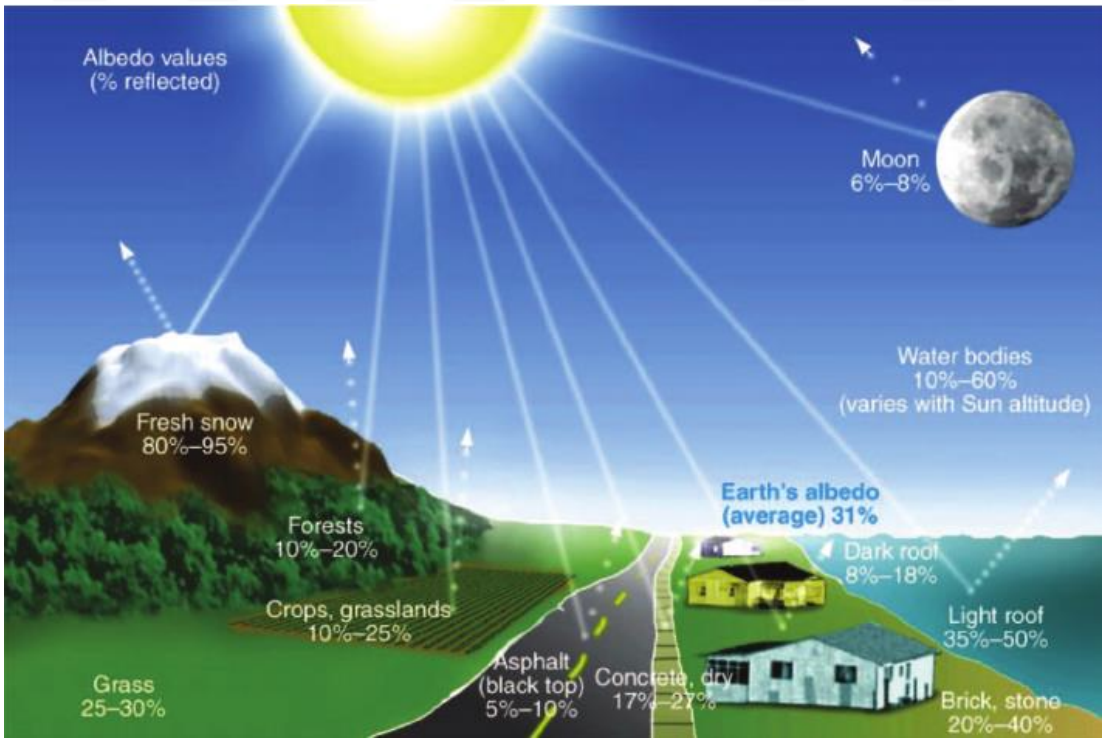

Figure 1.4. Albedo values of various surface materials (From sci.uidaho.edu)

CHAPTER 2
CHARACTERISTICS MODEL OF SOLAR CELL

Solar cells turn sunlight into electrical energy. The power of the sun, the solar constant, the power spectrum, and power losses in the earth's atmosphere are represented by the supposed air mass. The basic parameters of a photovoltaic cell are the short circuit current (I_{SC}), the open-circuit voltage (V_{OC}), the fill factor (FF) Eq,.(3) ,and the sun power altering efficiency (η) Eq.(4). Short-circuit current and open-circuit voltage are the highest current and voltage produced by a solar cell, respectively. The solar cell's power output is zero at both of these operational points. The "fill factor" or "FF", as it is more commonly known, is a parameter that, along with Voc and Isc, defines the maximum power of a PV cell. The FF is determined by the proportion of a PV cell's highest power to the product of Voc and Isc, such that:

$$FF = \frac{P_{MP}}{V_{OC}\, x\, I_{SC}} \qquad (2.1)$$

$$\eta = \frac{V_{OC}\ x\ I_{SC}\ x\ FF}{P_{in}} \qquad (2.2)$$

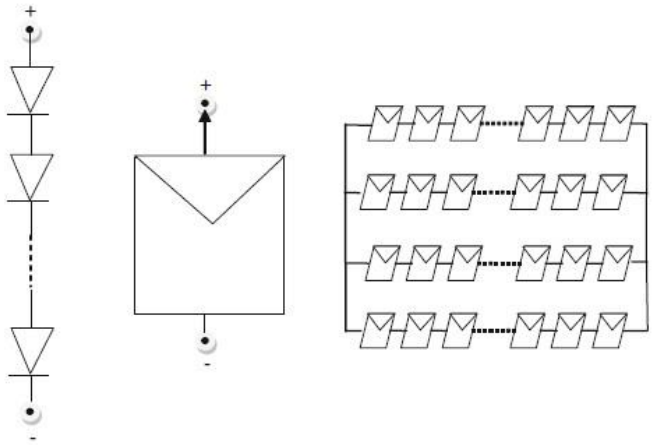

Figure 2.1. Cells, photovoltaic module, and panels (From Rekioua, D.)

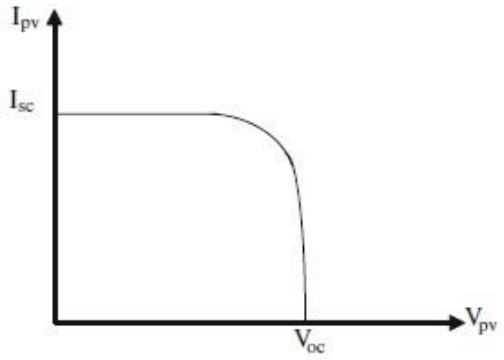

Figure 2.2. The typical form of I_{PV}-V_{PV} characteristic (From Rekioua, D.)

2.1 Maximum Power Point (MPP)

The power provided by a PV source is

$$P_{PV} = V_{PV}.I_{PV} \tag{2.1.1}$$

For the section of the I_{PV}-V_{PV} curve between the open-circuit and short-circuit points, and hence for V_{PV} values that match the criterion, this power is positive.

$$0 < V_{PV} < V_{OC} \tag{2.1.2}$$

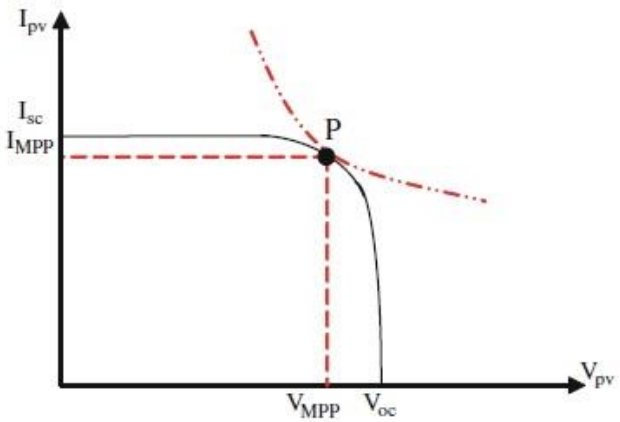

Figure 2.3. Current against voltage I_{PV}-V_{PV} graphic for a photovoltaic cell (From Rekioua, D.)

Outer of the interval described by Eq. (6), the power P_{PV} is negative, indicating that the PV device is receiving power from an external electric circuit. This scenario is not discussed in this section. The power P_{PV} is null when $V_{PV} = 0$ (short-circuit point) by Eq. (5) Similarly, P_{PV} is null when $V_{PV} = V_{OC}$ (open-circuit point) since, then

I_{PV} = 0 and thus, by Eq. (5), P_{PV} is also null. P_{PV} then reaches its greatest value inside the interval indicated by Eq. (6). This results in a point known as Maximum Power Point (MPP). V_{MPP} and I_{MPP}, respectively, are the corresponding values of V_{PV} and I_{PV} (Figure 2.3.). The power P_{PV} delivered by the photovoltaic generator is at its maximum at P(V_{MPP}, I_{MPP}) and is denoted P_{MPP}. We have:

$$P_{MPP} = V_{MPP}.I_{MPP} \tag{2.1.3}$$

With typical circumstances, the values P_{MPP}, $V_{MPP,}$ and I_{MPP} take sequentially the values $P_{MPP\text{-}ref}$ $I_{MPP\text{-}ref}$ and $V_{MPP\text{-}ref}$.

The MPP is reached when

$$0 = \frac{\partial P_{PV}}{\partial V_{PV}} \tag{2.1.4}$$

i.e., owing to Eq. (5),

$$0 = \frac{\partial (V_{PV} I_{PV})}{\partial V_{PV}} = I_{PV} + V_{PV} \frac{\partial I_{PV}}{\partial V_{PV}} \tag{2.1.5}$$

or equivalently,

$$-\frac{\partial V_{PV}}{\partial I_{PV}} = \frac{V_{PV}}{I_{PV}} \tag{2.1.6}$$

The left element of Eq. (10) is the incremental internal resistance of the PV generator (the negative sign is owing to the choice for that device of the generator reference directions). The load's apparent resistance is referred to as the right member. As a result, Eq. (10) can be thought of as the equation defining the resistance adaption of the load and the PV generator's internal resistance. For various situations, the current against voltage (Ipv-Vpv) and power against voltage (Ppv-*I*pv) curves are used to demonstrate the electrical characteristics of the PV cell.

2.2 Ideal Model

The simple equivalent circuit of a solar cell consists of a diode and a current source connected in parallel (Figure 2.4.). The photocurrent I_{ph} is produced by the current source and is proportional to solar irradiance G. The producer's datasheet provides the short-circuit current and open-circuit voltage, which are two key properties used to define a PV cell. The equation of the current voltage Ipv–Vpv facilitated equivalent circuit is created from Kirchhoff's law.

$$I_{PV}=I_{Ph} - I_d \tag{2.2.1}$$

Where

$$I_d= I_0\left[e^{q\frac{(V_{PV})}{AKT_j}} - 1\right] \tag{2.2.2}$$

Thus

$$I_{pv}= I_{Ph} - I_0\left[e^{q\frac{(V_{PV})}{AKT_j}} - 1\right] \tag{2.2.3}$$

I_{Ph} (A) is photo-current identical to the short-circuit current, I_0 (A) is the diode's reverse saturation current, q is the electron charge, K Botzman's constant, A is the diode ideality factor, T_j is the panel's junction temperature , Id is the current shunted through the intrinsic diode, and V_{PV} is the voltage across the solar cell.

$$I_{pv} = I_{sc} - I_0\left[e^{q\frac{(V_{PV})}{AKT_j}} - 1\right] \tag{2.2.4}$$

Setting I_{PV}=0 will give us the reverse saturation current I_0 (If the output current is not present)

$$I_{PV} = 0$$
$$V_{PV} = V_{OC}$$

$$0 = I_{Ph} - I_0\left[e^{q\frac{(V_{oc})}{AKT_j}} - 1\right] \tag{2.2.5}$$

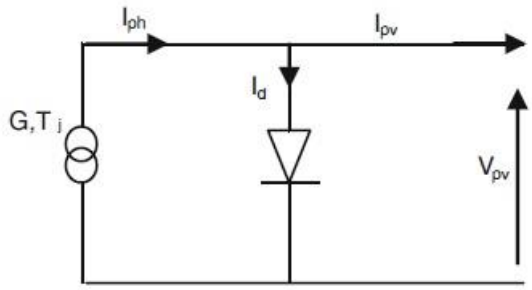

Figure 2.4. Simplified corresponding circuit of the photovoltaic cell (From Rekioua, D.)

Taking into mind that the photocurrent in this model is equal to the short-circuit current, we get:

$$I_0 = \frac{I_{sc}}{\left[e^{q\frac{(V_{OC})}{AKT_j}-1}\right]} \tag{2.2.6}$$

2.3 Model With Ohmic Losses

The second model accounts for physical resistance and ohmic losses because of degrees of contact to better describe the electrical condition of the PV cell in the ideal model. In the corresponding circuit, these losses are represented by a series of resistance Rs. (Figure 2.5.).

The following is the current voltage equation:

$$\text{Ipv} = \text{Iph} - I_0\left[e^{q\frac{(V_{PV}+I_{PV}.Rs)}{AKT_j}} - 1\right] \tag{2.3.1}$$

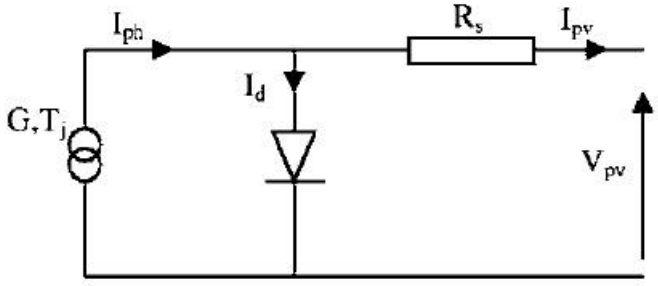

Figure 2.5. Simplified corresponding circuit of photovoltaic cell with R_S (From Rekioua, D.)

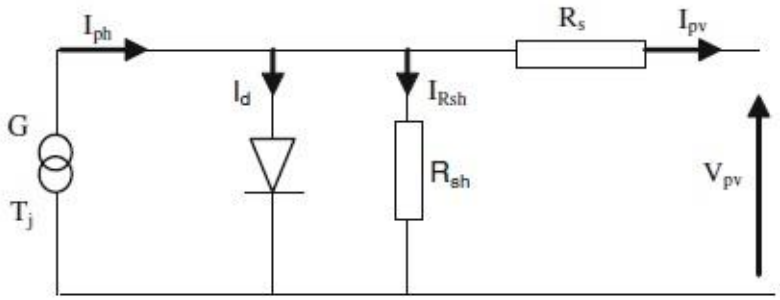

Figure 2.6. Simplified corresponding circuit of solar cell with R_{SH} and R_S (From Rekioua, D.)

An analogous circuit is used to define the first model discussed in this section. For the cell polarization phenomena, this one contains a single diode and two resistors (series and shunt) for the losses (Figure 2.6.). As a result, it is known as the "one diode design." Manufacturers use this design to describe the physical aspects of their PV cells (datasheets). The following equation describes the Ipv (Vpv) feature of this model:

$$Ipv = Iph - Id - IRsh \tag{2.3.2}$$

or, issue the terms Id and $IRsh$:

$$Ipv = I_{ph} - I_0\left[e^{q\frac{(V_{PV}+I_{PV}.Rs)}{N_{s-cell}KT_j}} - 1\right] - \frac{V_{PV}+Rs.I_{PV}}{R_{sh}} \tag{2.3.3}$$

2.4 The Two-Diode Model

The ideality factor n is assumed to have a constant value in the single diode equation. In reality, the ideality factor is determined by the device's voltage. When the device's recombination is dominated by the surfaces and bulk areas at high voltage, the ideality factor is near to one. However, at lower voltages, the ideality factor approaches two as recombination in the junction takes over. Modeling junction recombination involves connecting a second diode in series with the first and setting the ideality factor to two.

The two-diode model is a popular way of describing the basic characteristics of PV devices. Figure 1 shows the model's electrical equivalent circuit. The circuit also

includes a shunt resistance, two parallel diodes, a photosensitive current source, and a series resistance. The PV cell's terminal voltage and current may be connected mathematically as follows:

$$I=I_{PV}-I_{d1}-I_{d2}-\frac{V+R_sI}{R_{sh}} \quad (2.4.1)$$

This, using Shockley's diode equation, may be expressed as

$$I=I_{PV}-I_{01}\left[e^{\frac{q(V+R_SI)}{n_1KT}}-1\right]-I_{02}\left[e^{\frac{q(V+R_SI)}{n_2KT}}-1\right]-\frac{V+R_SI}{R_{sh}} \quad (2.4.2)$$

The photo current is *I*pv, the diodes' saturated currents are I_{01} and I_{02}, the diodes' model factors are n_1 and n_2, the charge of the electron is q, the Boltzmann stationary is k, and the p-n junction temperature is T in Kelvin. Additionally, R_S and R_{Sh} stand for series and shunt resistance, respectively.

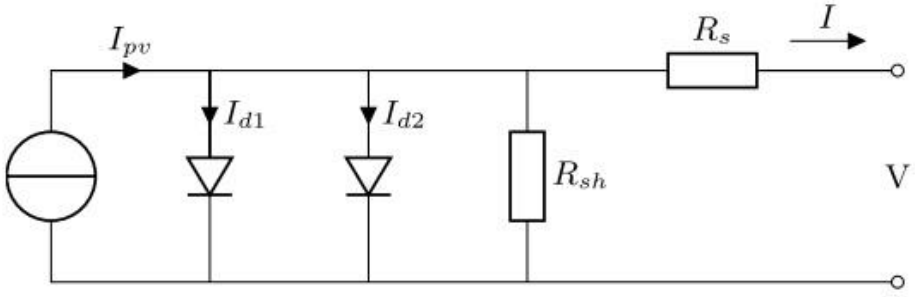

Figure 2.7. Electrical corresponding circuit of the two-diode PV model
(From Rekioua, D.)

2.5 Characteristics Curves of Solar Cells

2.5.1 Irradiance Effect

Figure 2.8 shows the solar cell's power–voltage (Ppv-Vpv) and current–voltage (Ipv-Vpv) characteristics for varying levels of radiation. The current (Isc) increases almost straight with irradiance, although the voltage Voc increases just a little. P_{MPP}

(Power-Maximum Power Point) thus grows rapid than the irradiance, implying that high irradiance improves efficiency.

Typically, 1,000 W/m^2 irradiance is used as the reference condition. In actuality, the irradiance on solar cell without light concentration is lower, and the efficiency is thus lower than the quoted number.

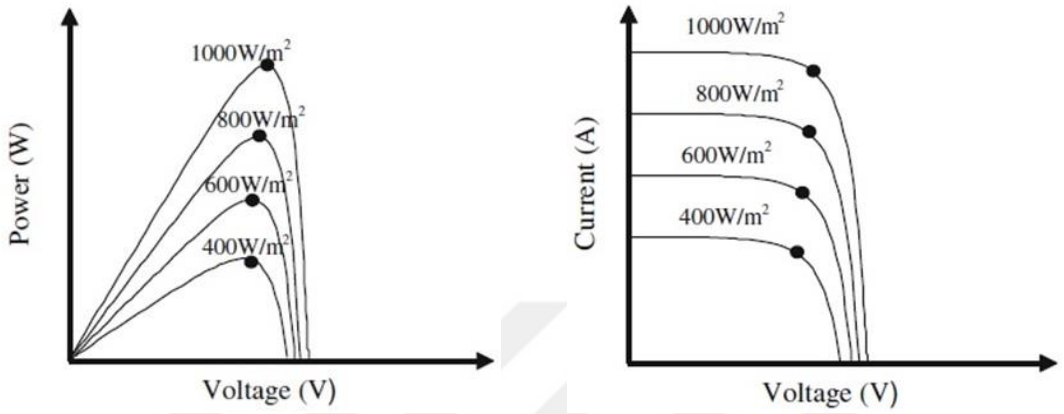

Figure 2.8. Irradiance influence on the electrical properties (From Rekioua, D.)

2.5.2 Temperature Effect

The short circuit current Isc increases marginally when the internal temperature Tj rises due to improved light absorption (because of that the energy decreasing with temperature), while the open-circuit voltage reduces dramatically. Temperature also has a significant impact (decreasing) on maximum electric power (Figure 2.9.).

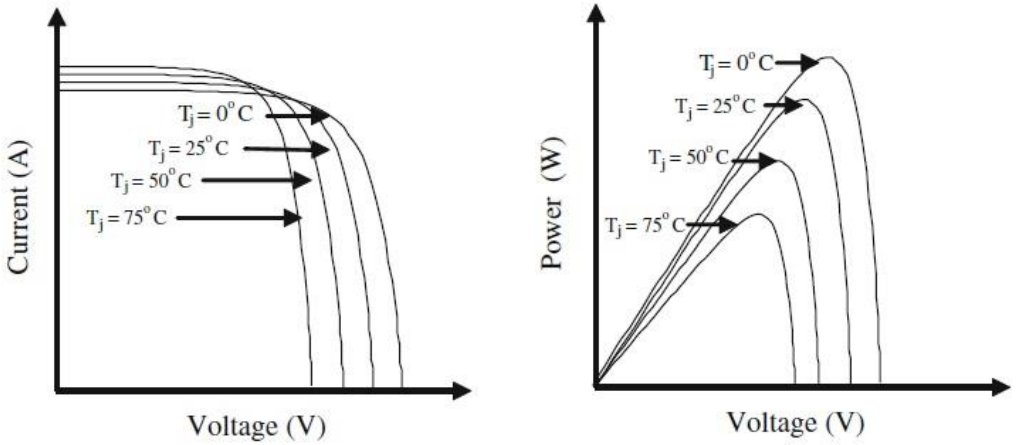

Figure 2.9. Temperature influence on the electrical properties (From Rekioua, D.)

CHAPTER 3
BIFACIAL PV MODULES, ALBEDO AND SOLAR RADIATION

3.1 Bifacial PV Modules and Albedo

The ground-reflected irradiance related to its albedo value possesses only a little influence on a typical PV system. Nevertheless, for a bifacial PV plant, albedo is critical. Figure 3.1. and Figure 3.2. demonstrate the correlative benefactions of the various components of the irradiances collected on the front and rear surfaces of a module. Although direct and diffuse components cancel out reflected irradiation in a standard PV plant, reflected irradiation is the predominant contributor to the irradiation gathered by the backside of the bifacial module.

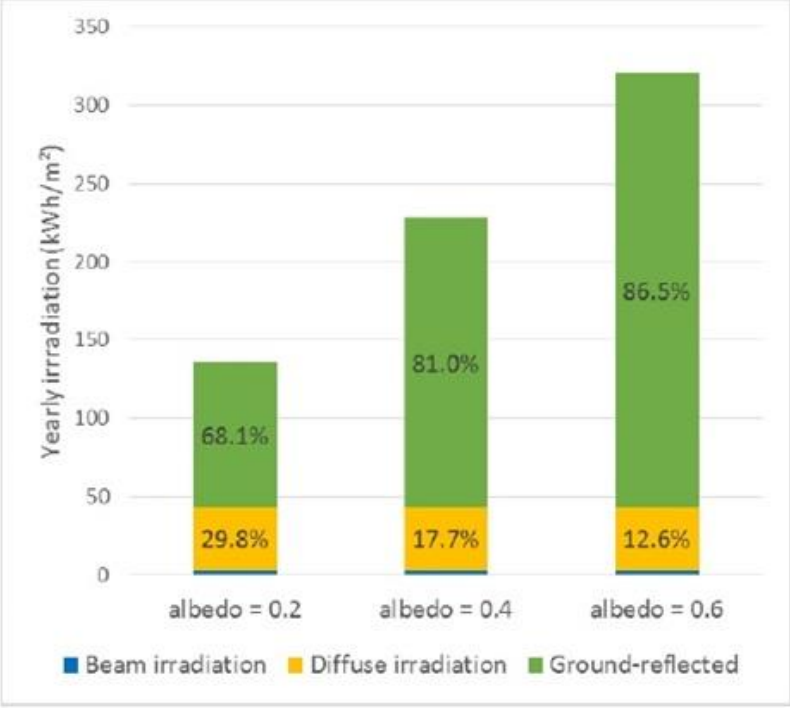

Figure 3.1. For different albedo values, the relative additions of light in the different components come to the rear surface of the PV module (From Chiodetti, M.)

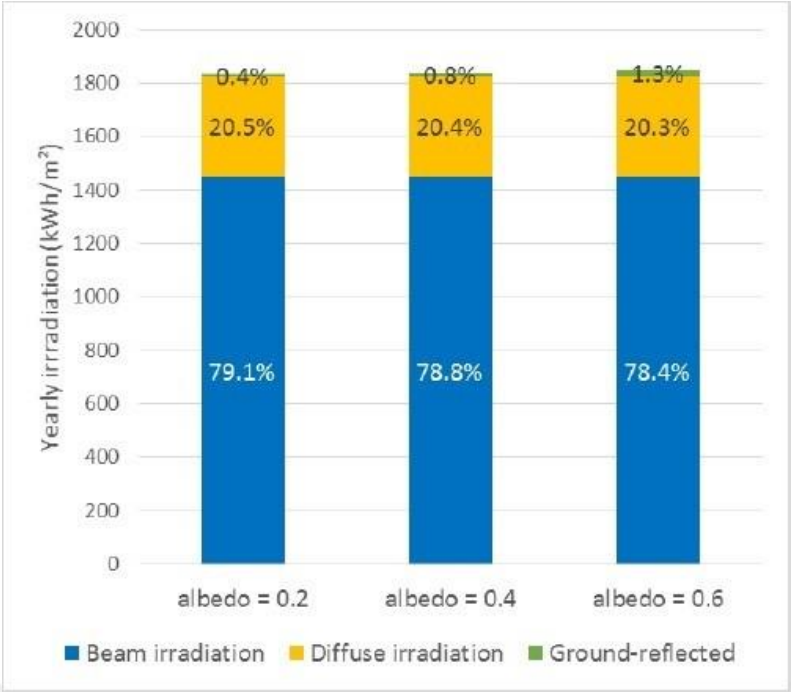

Figure 3.2. For different albedo values, the relative additions of light in the different components come to the front surface of the PV module (From Chiodetti, M.)

As well as pure climate-related factors such as solar radiation, temperature, wind speed, and precipitation (appearing as rain and snow), other site-specific factors will play a role in bifacial performance. One of the essential site-specific terms for bifacial modeling is ground reflectivity or albedo. Ground-reflected light is a need rather than an addition for bifacial applications. Albedo is critical even with monofacial PV when the tilt angle allows reflected light to contribute remarkably to the absorbed power inside the array's front-side surface This is critical in snowy high-latitude continental climates where sharp tilt angles are found. Because most natural surfaces absorb more light than they reflect, albedos typically vary from 15 to 30 percent, and natural materials have moderate to high reflection (e.g., water, white stone, snow). Constructed surfaces, such as crushed white stone, can be utilized to increase reflectivity. The albedo of a location can change dramatically throughout the year, owing to seasonal changes in soil moisture and vegetation and occasional brilliantly reflecting snow cover. Due to variable rock and soil forms and vegetation development, the albedo at multi-MW sites can vary considerably, making it critical to measure the albedo within the design to reach a bankable conclusion.

3.2 Direction of Beam radiation

Several angles can be used to describe the geometric relationships between a plane's orientation in relation to the earth at any given time (whether that plane is fixed or moving in relation to the earth) and the incoming solar radiation, or more specifically, the position of the sun in relation to that plane (Benford and Bock, 1939). Figure 3.3 shows the angles in some detail. The following are the angles and a set of uniform sign conventions:

φ **Latitude**, the angular location north or south of the equator, north positive; $-90^\circ \leq \varphi \leq 90^\circ$.

δ **Declination**, the angular position of the sun at solar noon (i.e., when the sun is on the local meridian) with respect to the plane of the equator, north positive; $-23.45^\circ \leq \delta \leq 23.45^\circ$.

β **Slope**, the angle between the plane of the surface in question and the horizontal; $0^\circ \leq \beta \leq 180^\circ$. ($\beta > 90^\circ$ means that the surface has a downward-facing component.)

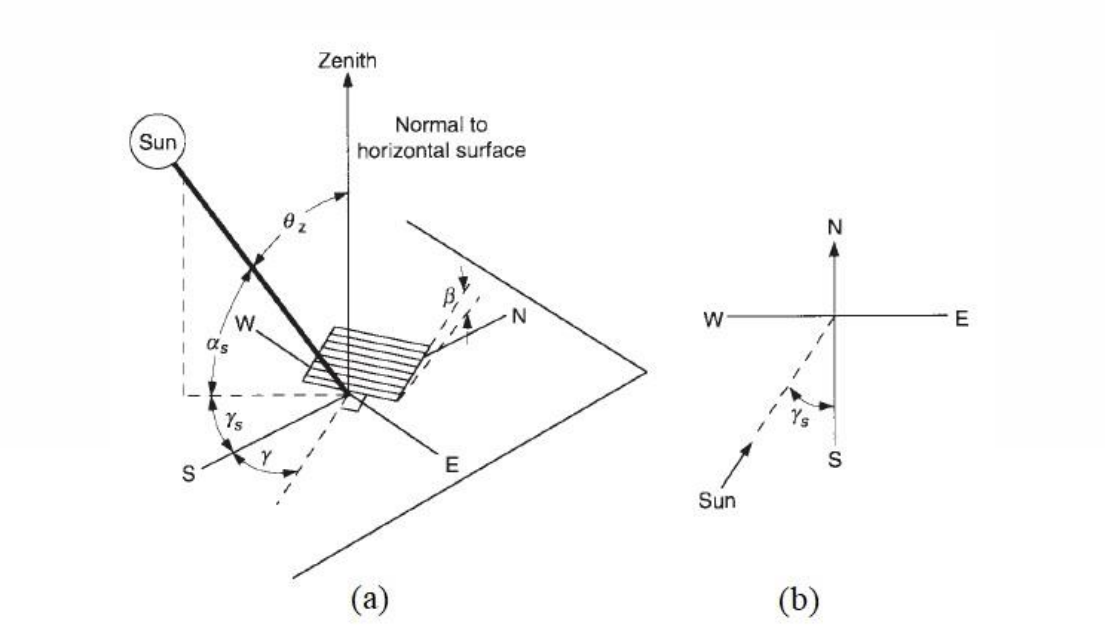

Figure 3.3 (a) Zenith angle, slope, surface azimuth angle, and solar azimuth angle for a tiltedsurface. (b) Plan view showing solar azimuth angle. (From Duffie, JA.)

γ **Surface azimuth angle**, the deviation of the projection on a horizontal plane of the normal to the surface from the local meridian, with zero due south, east negative, and west positive; $-180^\circ \leq \gamma \leq 180^\circ$.

ω **Hour angle**, the angular displacement of the sun east or west of the local meridian due to rotation of the earth on its axis at 15◦ per hour; morning negative, afternoon positive.

θ **Angle of incidence**, the angle between the beam radiation on a surface and the normal to that surface. Additional angles are defined that describe the position of the sun in the sky:

θz **Zenith angle**, the angle between the vertical and the line to the sun, that is, the angle of incidence of beam radiation on a horizontal surface.

αs **Solar altitude angle**, the angle between the horizontal and the line to the sun, that is, the complement of the zenith angle.

γs **Solar azimuth angle**, the angular displacement from south of the projection of beam radiation on the horizontal plane, shown in Figure 1.6.1. Displacements east of south are negative and west of south are positive.

The declination δ can be found from the approximate equation of Cooper (1969),

$$\delta = 23.45 sin(360 \frac{284+n}{365}) \quad (3.1.1)$$

There is a set of useful relationships among these angles. Equations relating the angle of incidence of beam radiation on a surface, θ, to the other angles are

$$\cos\theta = \sin\delta \sin\varphi \cos\beta - \sin\delta \cos\varphi \sin\beta \cos\gamma + \cos\delta \cos\varphi \cos\beta \cos\omega + \cos\delta \sin\varphi \sin\beta \cos\gamma \cos\omega + \cos\delta \sin\beta \sin\gamma \sin\omega \quad (3.1.2)$$

$$\cos\theta = \cos\theta z \cos\beta + \sin\theta z \sin\beta \cos(\gamma s - \gamma) \quad (3.1.3)$$

The angle θ may exceed 90◦, which means that the sun is behind the surface. Also, when using Equation 3.1.1, it is necessary to ensure that the earth is not blocking the sun (i.e., that the hour angle is between sunrise and sunset).

3.3 Radiation on Sloped Surfaces: Isotropic Sky

The combination of diffuse and ground-reflected radiation is isotropic, as suggested by Hottel and Woertz (1942). According to this supposition, the total radiation on the tilted surface is the sum of the beam contribution estimated as $I_b R_b$ and the diffuse on a horizontal surface, I_d. The diffuse from the sky and the ground-reflected radiation on the tilted surface are equal regardless of orientation. This is a step up from the presumption that all radiation can be handled as a beam, but there are still better options. Liu and Jordan developed the isotropic diffuse model as an enhancement to this model (1963). Three types of radiation were thought to be present on the slanted surface: a beam, an isotropic diffuse, and solar radiation that was diffusely reflected off the ground.

$$I_T = I_b R_b + I_d \left(\frac{1+cos\beta}{2}\right) + I\rho_g\left(\frac{1-cos\beta}{2}\right) \quad (3.2.1)$$

R_b =The Geometric Factor , ρ_g = Diffuse reflectance , I_b = Beam Radiation

I_d = Diffuse Radiation , I = Ground Radiation

I_T = Total Radiation (Mj/m^2)

I_T = Beam Contribution + The diffuse + Ground Reflected

3.4 Radiation on Sloped Surfaces: Anisotropic Sky

Improved models have been created that account for the horizon-brightening and/or circumsolar diffuse components on a tilted surface, which are schematically depicted in Figure 3.4. According to Hay and Davies (1980), who do not take into account horizon brightening, they estimate the proportion of the diffuse that is circumsolar and assume it all comes from the same direction as the beam radiation. The Hay and Davies model, originally proposed by Klucher (1979), is modified by Reindl et al. (1990b) to include a horizon brightening element, creating the HDKR model.

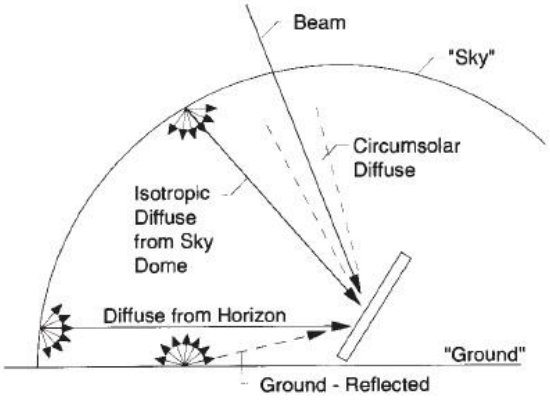

Figure 3.4 Beam, diffuse, and ground-reflected radiation on a tilted surface. (From Duffie, JA.)

$I_{d,T} = I_{T,d,iso} + I_{T,d,cs}$, I_o =Beam Radiation

$A_i = \frac{I_{bn}}{I_{on}} = \frac{I_b}{I_o}$ (A_i is an **anisotropy index** which is a function of the transmittance of the atmosphere for beam radiation.).

The total radiation on a tilted surface (The Hay-and-Davies model) is then

$$I_T = (I_b + I_d A_i)R_b + I_d(1 - A_i)\left(\frac{1+cos\beta}{2}\right) + I\rho_g(\frac{1-cos\beta}{2}) \qquad 3.3.1$$

The HDKR model (the Hay, Davies, Klucher, Reindl model) produces the findings after adding the beam and ground-reflected factors. The total radiation on the tilted surface is thus,

$$I_T = (I_b + I_d A_i)R_b + I_d(1 - A_i)\left(\frac{1+cos\beta}{2}\right)\left[1 + fsin^3(\frac{\beta}{2})\right] + I\rho_g(\frac{1-cos\beta}{2}) \qquad 3.3.2$$

$$f = \sqrt{\frac{I_b}{I}}$$

3.5 The Future of Bifacial PV Modules

Based on the ITRPV (International Technology Roadmap for Photovoltaics report), research forecasted that the wholesale share of bifacial solar modules will expand from 10% in 2020 to 35% by 2030. According to market forecasts, the bifacial PV market would treble by 2030 in Figure 3.5. Depending on installation and location conditions, they will have an increase in power of 5% to 30% over monofacial panels. The majority of PV panels on the wholesale are monofacial PV cells, but bifacial PV cells could be used for monofacial and bifacial PV panels. Approximately 50-60% of bifacial PV cells will be used to build bifacial modules, whereas 40-50% will be put into monofacial modules, based on ITRPV's estimates.

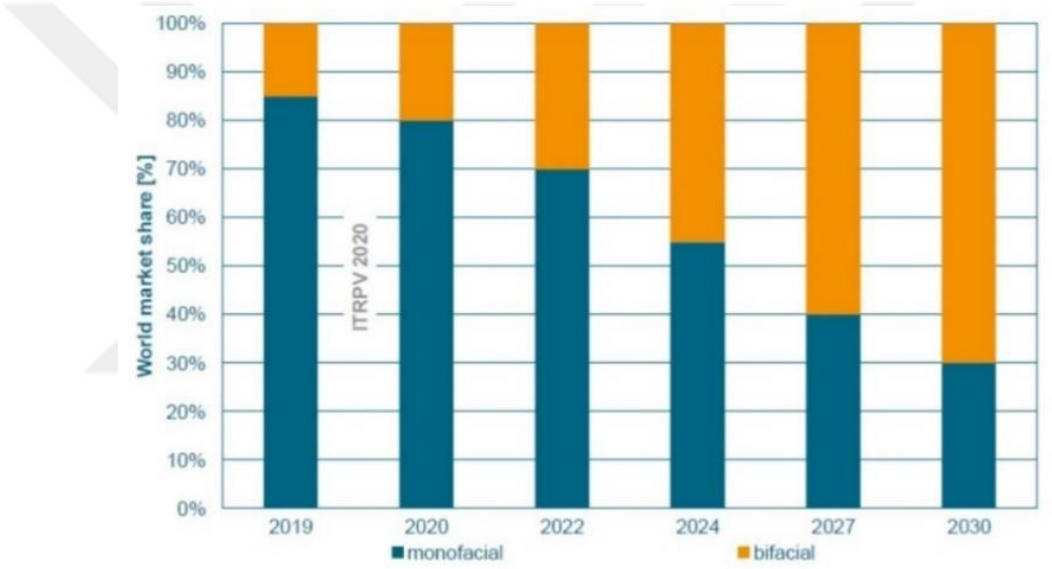

Figure 3.5. The ratio of photovoltaic cells in the PV trade of the ITRPV 2020 (From Kopecek, R.)

One of the primary projected causes for the bifacial module market share to continue to grow is seen in Figure 3.6. The higher costs associated with generating the backside of bifacial modules can be balanced when bifacial production increases (with more data reachable and better designs obtainable). Several factors must be taken into account when calculating the cost of the bifacial plant and forecasting its power output. In comparison with monofacial modules, bifacial modules would generate an extra 10%-20% of power. The Increased capacity can be around 30-40% more if circumstances are improved and single-axis trackers are used.

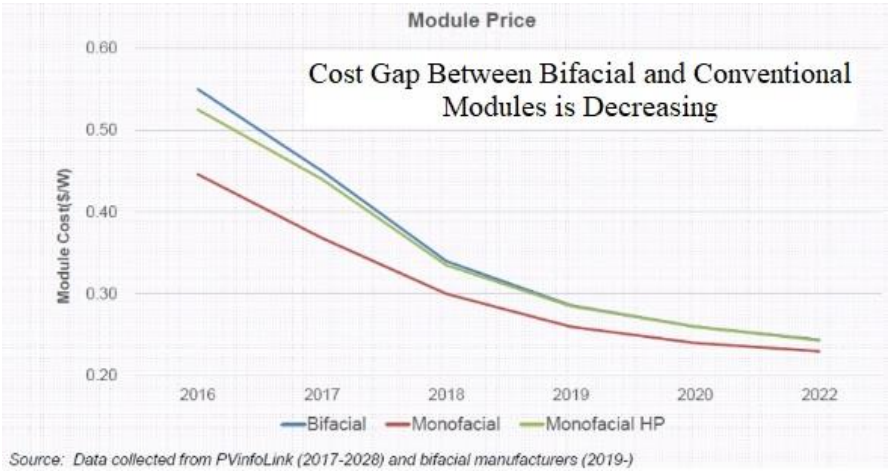

Figure 3.6. The Price gap between bifacial and monofacial panels (From Lusson, N.)

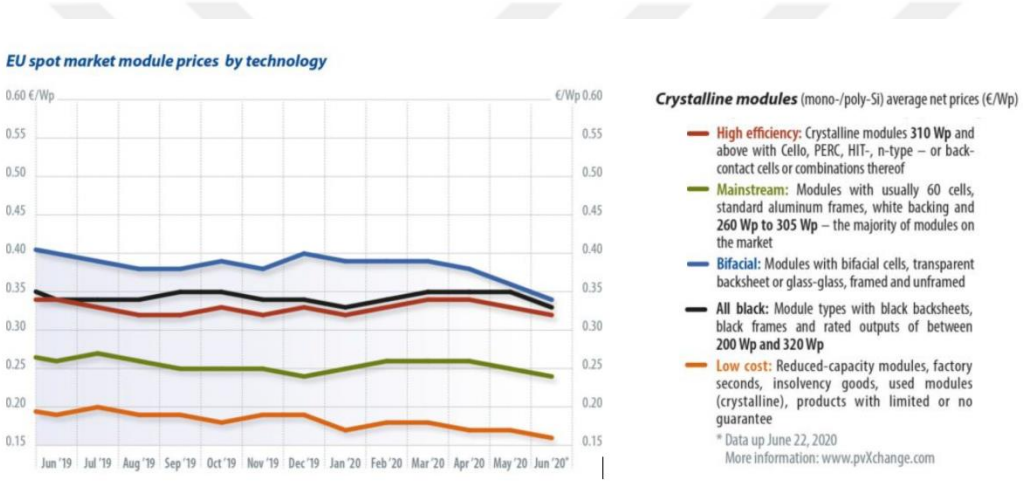

Figure 3.7. EU spot market panel costs by technology (From Lusson, N.)

If the cost gap narrows and bifacial production grows (indicating more data accessibility and better design), the higher manufacturing costs of generating the backside of bifacial modules may compensate for additional expenses. Is increased manufacture, however, sufficient to pay the higher costs? The solution is complex. While the increased equipment and installation costs of bifacial PV plants aren't high, there are other issues that limit their use. As a result of many design characteristics unique to bifacial systems, the overall installation costs are higher, especially on backsides of panels. A bifacial plant's DC design, site placement, and installation might be more difficult than one with monofacial modules, which can cause challenges for investors. Because of the multiple variables that influence rear side production, it is also hard to predict the enhanced output for a system layout (Figure 3.7).

CHAPTER 4

TURKEY'S PHOTOVOLTAIC POWER POTENTIAL

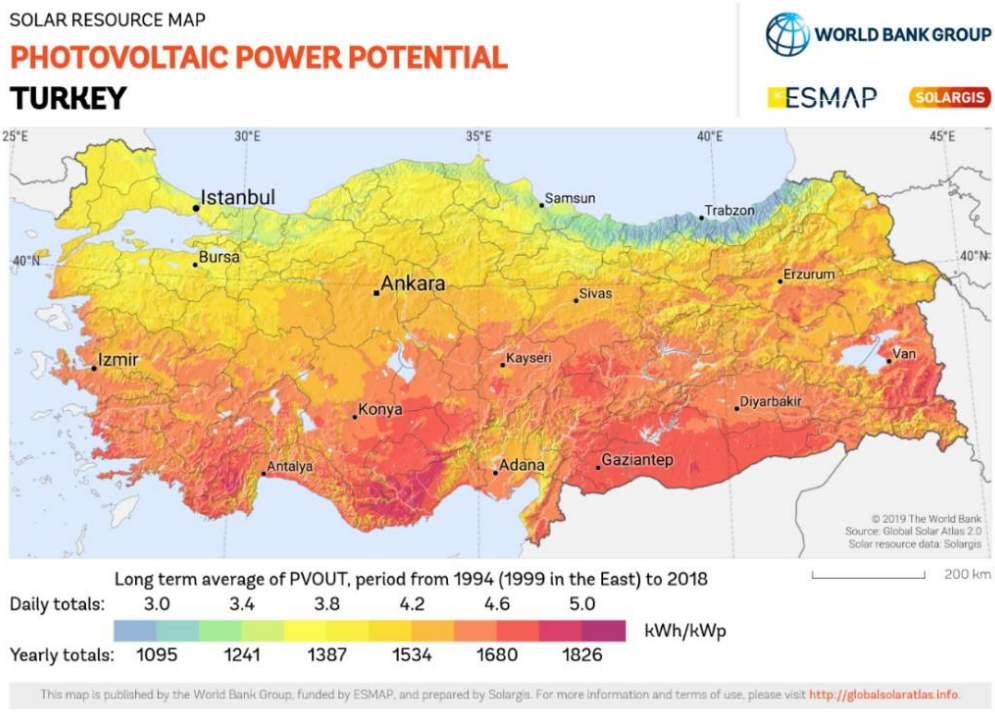

Figure 4.1. The PV power potential of Turkey (From Solargis.com)

Turkey is located in a unique position in the Middle East and Southeast Europe for solar energy. About 5% of Turkey's electricity will be generated by solar energy by the end of 2022, when there will be almost 10 GW of solar power plants (see Figure 4.2). Solar potential is excessive in Turkey, particularly in the South Eastern Anatolia and Mediterranean provinces in Figure 4.1. Turkey is Europe's largest solar panel manufacturer and the world's fourth, to break into the top three next year. Turkey's electric power generating capacity has tripled to more than 100 GW since 2002, with renewables accounting for 54% of total capacity, up from 38% in 2002. Since 2014, solar power has grown the most, from 40 MW to over 8 GW. Karapınar solar power facility in the Konya province is Turkey's largest solar project. By the end of 2022, total nameplate capacity (direct current) is expected to reach 1.35 GW. It converts to 1 GW of alternating current (AC), the maximum amount of power that the

plant can deliver to the transmission network. Karapınar is on track to become the world's sixth-largest power station by capacity, and the largest in Europe. Turkey's sun radiation and installation length are seen in Table 1.

Table 1. Average daily solar radiation and insolation length vary monthly in Turkey (MENR 2021b)

Month	Average daily solar radiation (kWh/m^2-day)	Average daily insolation duration (hour/day)
January	1.79	4.11
February	2.5	5.22
March	3.87	6.27
April	4.93	7.46
May	6.14	9.1
June	6.57	10.81
July	6.5	11.31
August	5.81	10.7
September	4.81	9.23
October	3.46	6.87
November	2.14	5.15
December	1.59	3.75

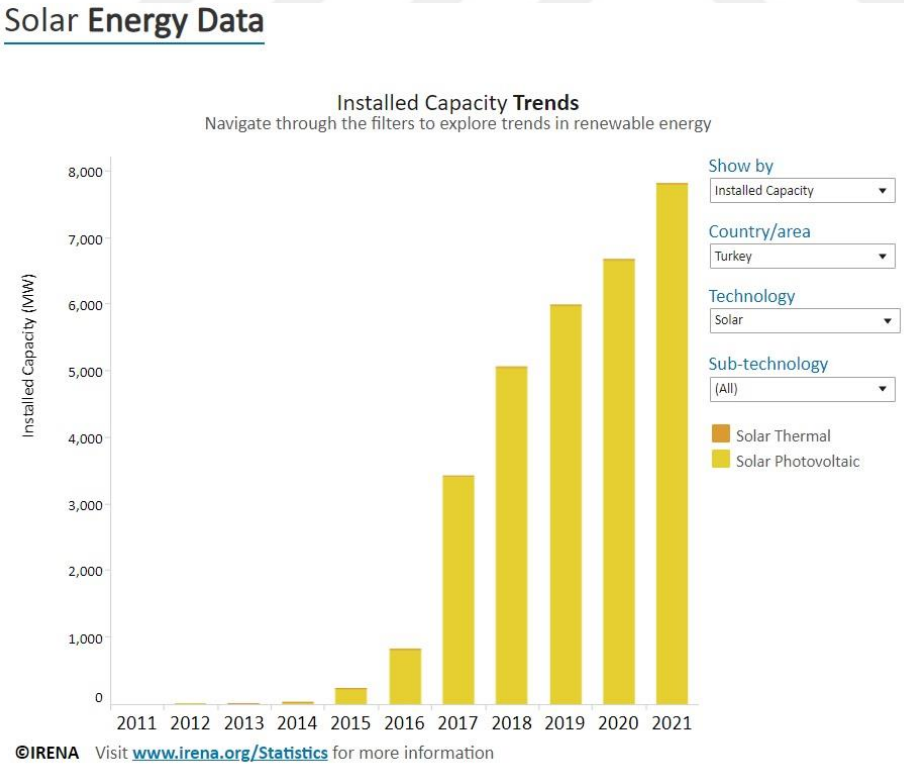

Figure 4.2. The solar installed capacity trends of Turkey (From IRENA)

CHAPTER 5
WHAT IS PVSYST SOFTWARE

PVsyst is an international criterion for solar system design and simulation, created by A. Mermoud and M. Villoz. It is claimed that this software is designed and simulated to be used by researchers, students, architects and engineersA solar simulation program known as PVsyst is commonly used for estimating power production and deciding on optimal designs for solar power plants (See Figure 5.1.). It provides a comprehensive contextual help menu that describes the techniques and models utilized, as well as a user-friendly manner with a project construction guide. PVsyst has in-depth understanding of solar technology, resource data of meteorological irradiation, and solar system components. As a result, it will aid in understanding the PV system components and hence in optimizing the system design. There are a lot of solar design simulation software on the market, such as Helioscope, Aurora, etc. However, PVSyst is accepted almost globally and is one of the oldest software. It is quite comprehensive and provides excellent results for larger utility-scale projects. PVSyst as a solar design software is exceptionally feature-loaded and complex.

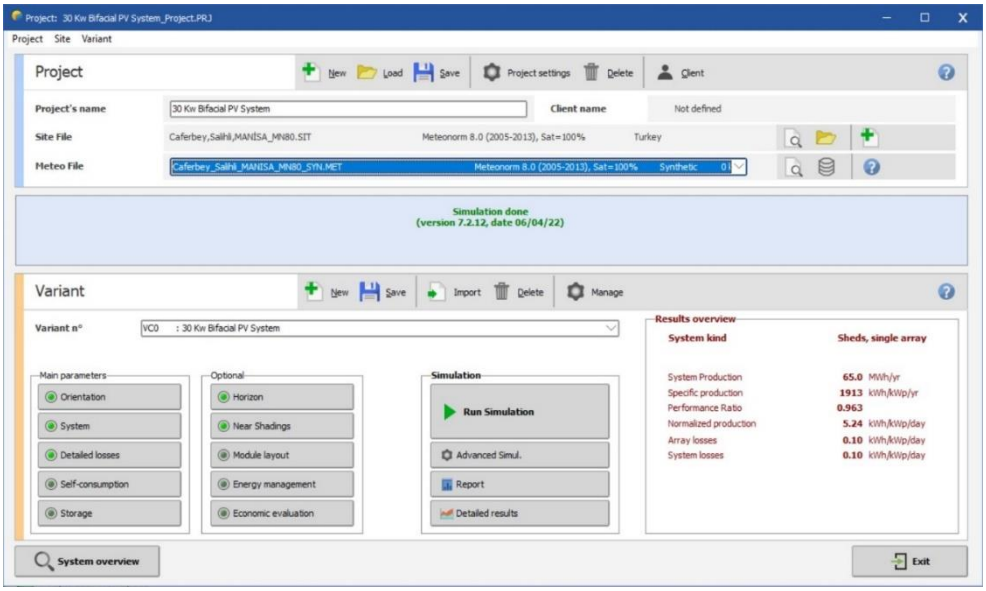

Figure 5.1. The PVsyst software design

Preliminary and Project Design solar simulations are available from PVsys.

- A quick estimating tool is a **preliminary design**. Because you can generate pre-sale designs in minutes, it's ideal for them**.**
- Engineers will model lucrative solar systems during the **project design** phase. A lot of criteria and choices are needed in these designs. Engineers will have higher trust in their simulated output after gathering more best-standing data.

5.1 To develop and simulate PVsyst models, which systems may be used?

Grid-connected systems: Grid-connected systems are the most commonly used simulation instrument. Simulations may be run at every stage of a process to determine energy conversion and losses. All simulation results include expected energy output, performance ratios, and financial measures. You may create both commercial and multi-megawatt PV tracking systems.

Stand-alone systems: Off-grid or stand-alone to replace the grid, systems rely on batteries and generators. You must be aware of comprehensive energy expenditures as well as a day to day energy profile per-hour because these systems are complicated. PVSyst, for instance, could construct stand-alone PV systems with high, medium, and low power in a fairly wide range.

Pumping systems: Solar pumps are commonly utilized in agriculture. Modules mounted on single-axis trackers have recently become widespread, allowing this technology to be used in design workflows. PVSyst provides a summary of water requirements, pump energy, pumped water, and pump efficiency.

DC Grid: Project Designs are the just place where you may use DC Grid.

5.2 How does PVsyst Software differ from other products?

System Scaling: PVsyst has a Visual Tool for scaling and balancing systems. It is critical to discern the many components of a system and determine where further work ought to be done. PVsyst provides real-time data on the scale and limits of your system. You may also choose which states the system will activate.

System Design: System design environment provides you with all over necessary information in an easy-to-follow format so that you can start designing your system immediately.

Simulations, Reports, and Economic Evaluation: Several simulation capabilities are available to users, providing regular updates and energy levels on the system in chosen areas throughout the assignment. With PVsyst, operators can see how the entire system is performing in real-time, improving their understanding of the whole system.

5.3 PVsyst Tools

Outside of a PVsyst simulation, we may employ five solar instruments and four data analysis techniques.

- **Solar Parameters Tables:** Hundreds of variables may be tracked using this program.
- **PV Arrays Tool or Electrical Behavior:** Analyzes shading effects at the cell level by using this tool.
- **Factor Tool for Transfer:** This method is applied to calculate how much energy can be captured by solar modules that are tilted.
- **Meteorological Calculator - Monthly:** In this case, solar irradiance is calculated rapidly, such as Apex Sun Hours / Monthly kWh.
- **Utilizing the Voltage Improving Tool:** An MPP tracker may not be the ideal option in some tiny solar setups. This tool assists in making decisions.

Data analysis software may also assist in cleaning and transforming large data volumes. It is critical to ensure that meteorological data is accurate and faultless.

5.4 PVsyst: What are the Benefits for Solar PV Creators?

Professional PV system designers and installers can take an edge in an increasingly crowded field with PV system design software like PVsyst. With PVsyst, customers can manage their solar panels with equipment and software in one place, simplifying the process for consumers. Here are several significant advantages:

Built-In Meteorological Data:

Solar radiation data is not only imported into PVSYST, but it as well comes with a NASA and Metenorm data interface ,so you won't have to worry about not having accurate solar statistics. Weather data can be obtained anywhere and anytime using Meteonorm, a third-party program that supplies thousands of sites worldwide with a huge database of meteorological information. Meteonorm makes it simple to get weather data anywhere, at any time. With a few clicks, you may create a fake hourly weather file.

Huge Hardware Library:

The hardware library has thousands of pumps, generators, batteries ,inverters, and solar panels. These make it simple to use market-available items and are updated regularly. In addition, PVSyst includes numerous features that allow for the importation/addition of the latest solar PV panels, inverters, and other components. For example, PVSyst supports the import of new panels from the modules .pan file in case Sunpower publishes one.

Powerful Simulations:

PVsyst lets you examine overall system performance and simulate your energy use in real-time on any given day. With just one click, your electricity consumption, battery bank the amount of energy it receives and the amount of electricity required by each system component can be learned.

3D Shading Scene Analysis:

PV system designers must consider shadow effects on panels as one of the most important decisions. PVSyst could form to build a 3D shading place that mimics shading objects and energy losses.

PVsyst is a very strong piece of software that is also not the easiest to understand. A solar simulation has hundreds of parameters that must be entered. It's one thing to understand how to utilize the program. Finding which inputs should be fed into the model poses another challenge**.** The smart solar designer understands inputs should be based on reliable data and, when necessary, produce accurate estimates. As they say in simulations, "garbage in, trash out.".

CHAPTER 6
30-KW BIFACIAL PV SYSTEM DESIGNING WITH PVSYST

A 30-kW bifacial PV system was designed and simulated with PVsyst software to see the albedo effect in a bifacial photovoltaic system. The 30 kW solar covered area can give enough data to analyze and assess the results of the albedo effect. We should also know that a 30 kW PV system provides sufficient operating power for many individuals and small businesses.

6.1 Geographical Area Parameters and Horizon Line Drawing for Caferbey, Salihli, MANİSA

The meteorological data is the first step consideration of a project. The project's geographic coordinates are taken from Meteonorm 8.0 database for Caferbey, Salihli, Manisa, TURKEY, and located at the latitude of 38.4772 N and the longitude of 28.0972 E at an altitude of 126 meters. This geographical area is chosen because it is suitable for setting up the project. Geographic area parameters are seen in Table 2.

Table 2. Geographic area parameters for Caferbey, Salihli, Manisa, TURKEY

	Global horizontal irradiation	Horizontal diffuse irradiation	Temperature	Wind Velocity	Linke turbidity	Relative humidity
	kWh/m²/mth	kWh/m²/mth	°C	m/s	[-]	%
January	68.2	31.7	6.6	2.19	3.269	77.6
February	77.2	39.7	8.3	2.41	3.710	74.1
March	125.6	61.2	11.6	2.39	4.355	66.3
April	164.8	74.6	15.6	2.19	4.930	60.9
May	209.4	77.5	21.1	2.30	4.501	54.5
June	229.4	73.0	25.8	2.70	3.851	47.5
July	240.1	64.8	29.5	3.10	3.735	42.6
August	215.0	59.1	29.2	3.10	3.790	44.9
September	163.9	50.1	23.9	2.39	3.689	52.5
October	115.7	46.0	18.4	2.10	3.719	62.0
November	76.9	33.1	12.7	1.90	3.469	73.0
December	59.9	24.6	8.1	2.00	3.301	76.4
Year	**1746.1**	**635.4**	**17.5**	**2.4**	**3.860**	**61.0**

Global horizontal irradiation year-to-year variability 5.4%

Caferbey,Salihli,MANİSA (Turkey)

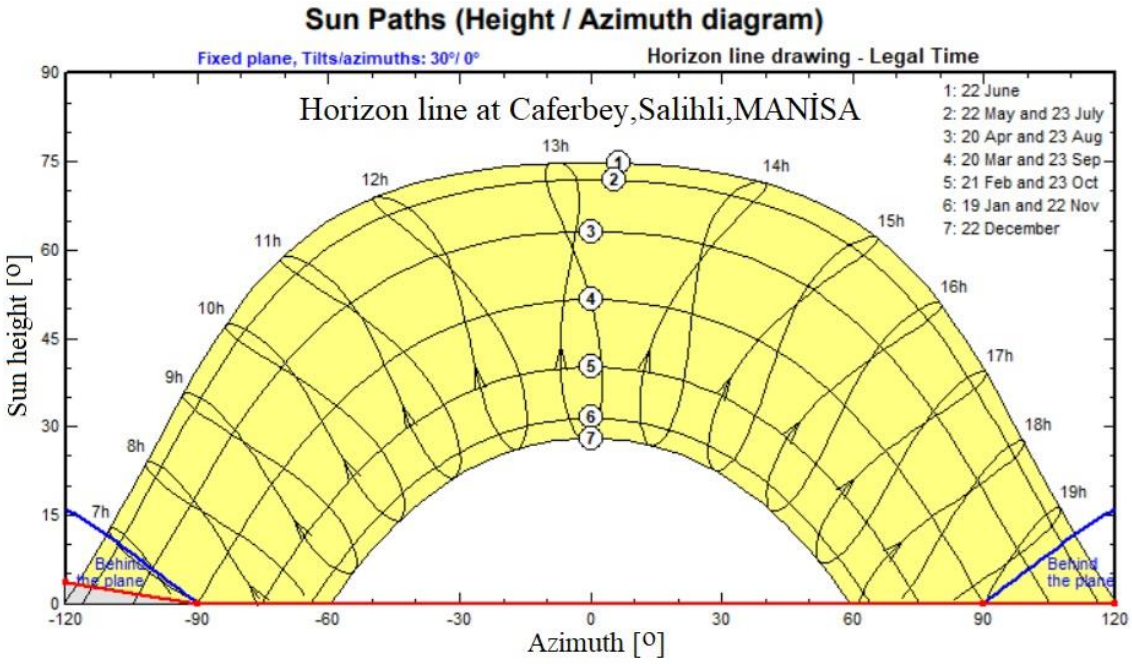

Figure 6.1. Horizon line at Caferbey,Salihli,Manisa,TURKEY by PVsyst

The horizon of the far shadings section is the uncomplicated way of defining shadings in PVsyst (See Figure 6.1.). However, this is only suitable for considering shadings of objects that are adequately far away since we may consider them to operate on the PV field globally: the sun is either visible or not visible on the field at any one time. Typically, the spacing between these shading objects should be greater than ten times the size of the PV field.

6.2 Designing and Shading Scene Construction

Firstly, we need to define the PV system mounting system. There are three different solar PV mounting systems: Fixed-mount type, single-axis tracking, and dual-axis tracking. We chose the fixed mount type for this project because the costs of investment, maintenance, and application are easy to handle for others way. For stationary mount type, the tilt angle is taken as the optimum value of 30° for obtaining maximum irradiance seen in Figure 6.2. And also, for the same reason, the azimuth angle is taken at 0° degrees.

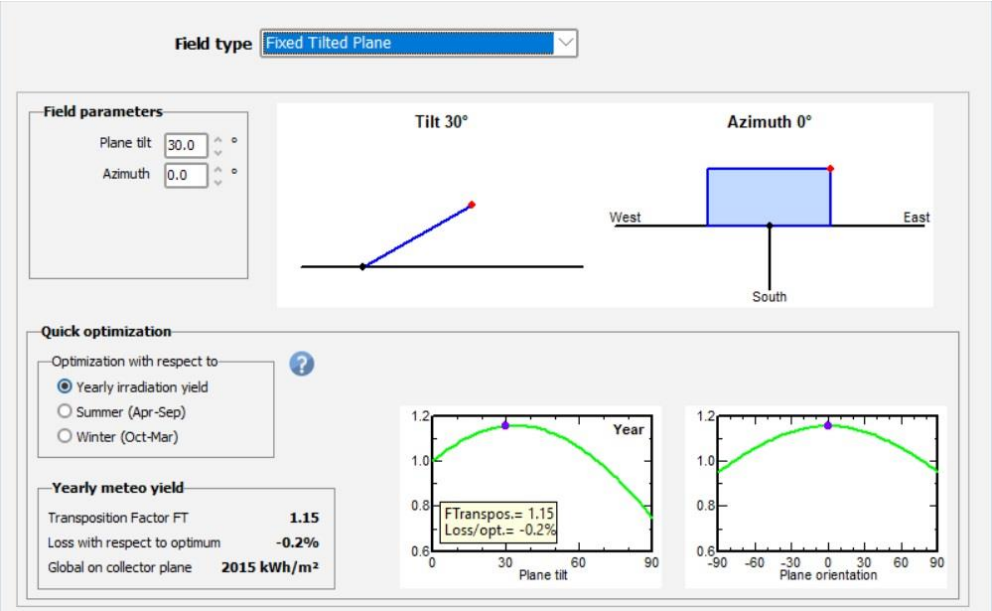

Figure 6.2. Orientation, variant " 30 Kw bifacial PVsyst. "

While designing a 30 kW PV system, 80 units of 425-watt PV modules were used. Eighty modules were used in 4 rows, 20 of which are in each row. The pitch value (inter-row spacing) was taken at 5 m. Also, the panel's elevated height was taken at 1.35 m. These parameters were taken for the optimum values for covering fewer spaces but gaining a high yield. Shading scene construction is shown in Figure 6.3.

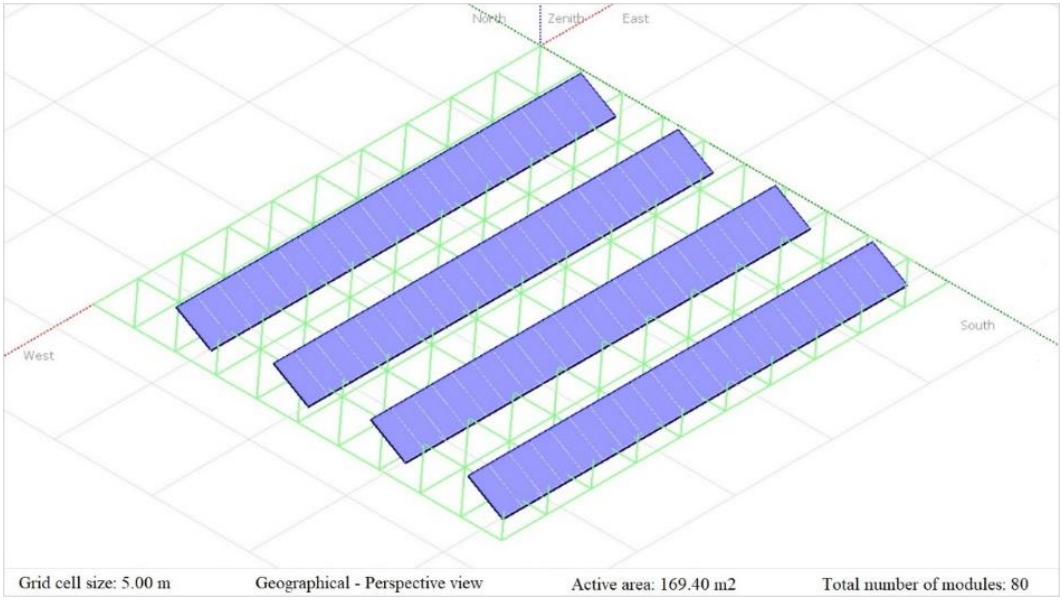

Figure 6.3. Shading scene construction by PVsyst

6.3 The PV module Selection

Bifacial modules are used to analyze the albedo effect on the PV system in this project.

PV modules are available in a range of sizes and forms, each with its unique set of characteristics. Among these modules, a highly efficient, widely available, affordable, and the local product was selected. Selecting a high power and efficiency PV module ensures less use of the surface area. The selected PV module is seen in Figure 6.4.

Figure 6.4. Selecting the Pv module by PVsyst

The chart of proficiency against the occurrence sun oriented radiation under fluctuating temperature conditions is displayed in Figure 6.5, which exhibits that as the temperature increments of the PV module, the effectiveness diminishes at a particular radiation level. The efficiency of the solar panel is 20.47 % at STC. It is clear from Figure 6.6., that as the occurrence sunlight based radiation level ascents, the greatest current for a PV module likewise rises and less affects the voltage when the temperature stays stable.

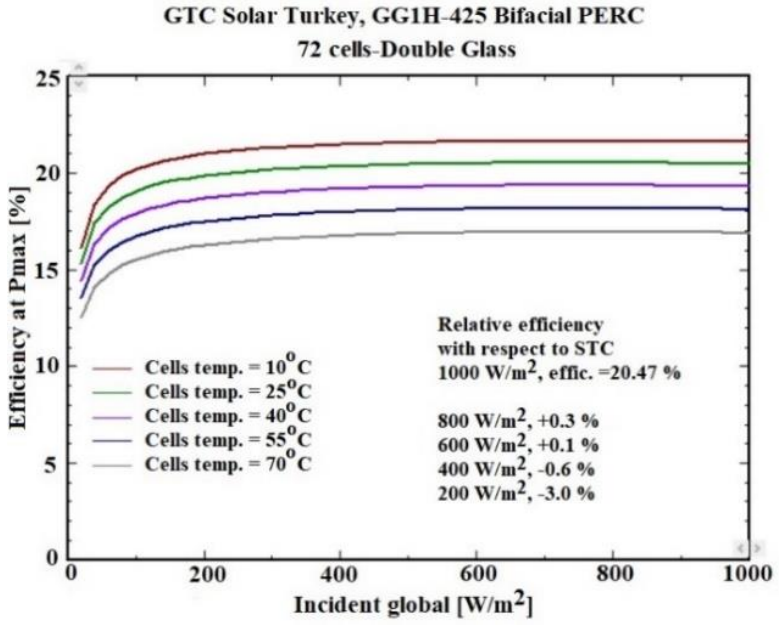

Figure 6.5. Efficiency at Pmax [%] vs. incident global [W/m^2] of GTC panel

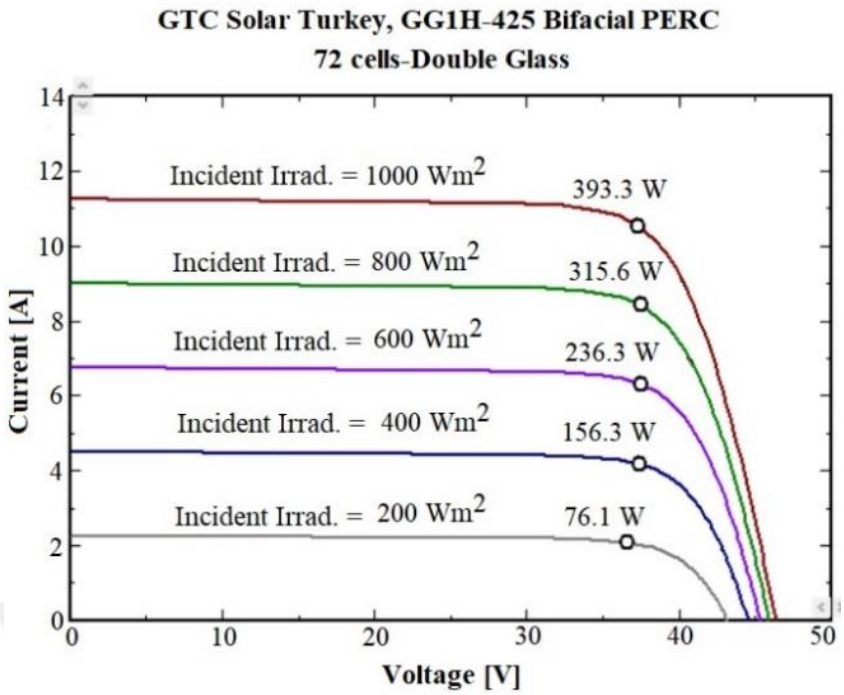

Figure 6.6. Current [A] vs. voltage[V] of GTC panel

6.4 The Inverter Selection

An inverter is one of the essential pieces of equipment in a solar energy system. Our sample 30 kW PV system uses two inverters of 15 kW AC output power and two MPPT inputs. The inverters' operating points and electrical conditions must be consistent with the PV system, as the operating DC voltage of the inverter should not exceed minimum and maximum operating values. The selected inverter is shown in Figure 6.7.

Figure 6.7. Selecting the inverter by PVsyst

The PNom ratio is the proportion of installed PV power (DC) (nominal at STC) to inverter nominal AC power. This is truly a widely-used reference when sizing the inverter. It is often determined to get an insignificant overload loss. Pnom ratio was taken at 1.13 in this project. The other important parameter in this section is Voc (-10 ^{o}C). It should be a lover than the maximum dc voltage of the inverter. The designed array is shown in Figure 6.8.

Figure 6.8. Designing the array by PVsyst

6.5 Schematic of 30- kW Bifacial PV System

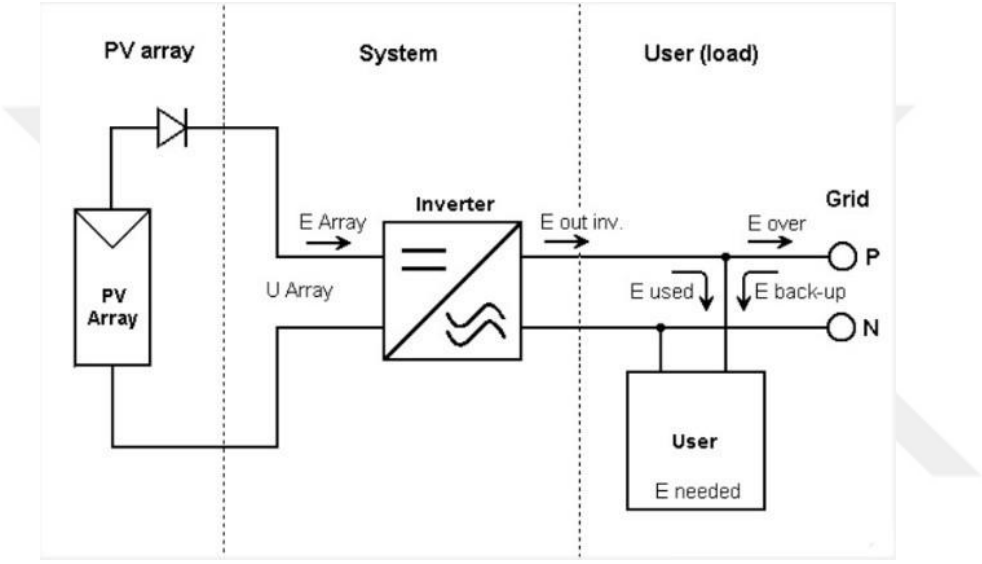

Figure 6.9. Schematic of 30-kW bifacial PV system

A grid-connected system is depicted in Figure 6.9. A clarified block diagram with three primary components: the PV array, the ultimate users load and inverters. Firstly, a PV array collects solar radiation and converts it into electricity with a DC current that flows through the system. Secondly, an inverter is taken to change over the DC current into AC current that the system's instruments can utilize. Finally, any surplus power is sent to the grid.

6.6 Beam and Diffuse on The Ground with Sheds

The beam and diffuse on the ground with shed graphics are shown in Figure 6.10. On the left side, there are design parameters. Ground albedo is chosen at 0.65. This value can be achieved easily with white paint or white portland cement.

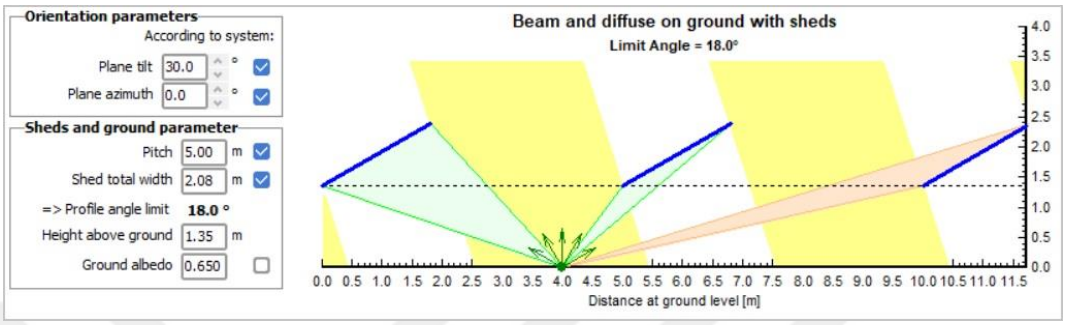

Figure 6.10. Beam and diffuse on the ground with sheds by PVsyst

CHAPTER 7
30-KW BIFACIAL PV SYSTEM SIMULATION RESULTS AT PVSYST

The 30-kW bifacial PV system, which initial definitions and designs are made above, is simulated in the next section. Simulations for critical parameters were made with PVsyst software, and the results were obtained in the table form. As a result of the simulations, the correlation of the albedo effect with the bifacial modules is examined in Table 2. In today's conditions, bifacial modules will be discussed in the conclusion section considering the albedo effect.

7.1 Optimization Tool Results

The PVsyst software is also used to determine the appropriate tilt angle and azimuth built in the system definition and to ensure that it is acceptable and efficient for this system using software simulation. The optimum tilt is 30^{o}, and the azimuth is 0^{o} to the south, as seen in Figure 7.2. below. The maximum power capacity of our system can be produced at this tilt and azimuth angle. Also, PVsyst's software helps us to find optimum values of Height, GCR, and Pitch step-by-step graphics using an optimization tool. Elevation height and E_Grid graphics can be seen in Figure 7.3. Elevation height was taken at 1.35 m. GCR and E_Grid graphics can be seen in Figure 7.4. GCR was taken % at 41.6. Pitch and E_Grid graphics can be seen in Figure 7.5. Pitch is taken 5 m. Tilt vs. pitch optimization result is seen below (Figure 7.1.).

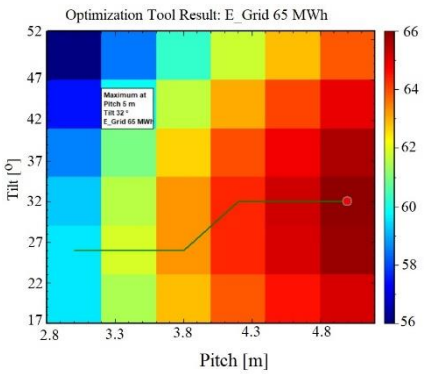

Figure 7.1. Tilt vs. pitch optimization result

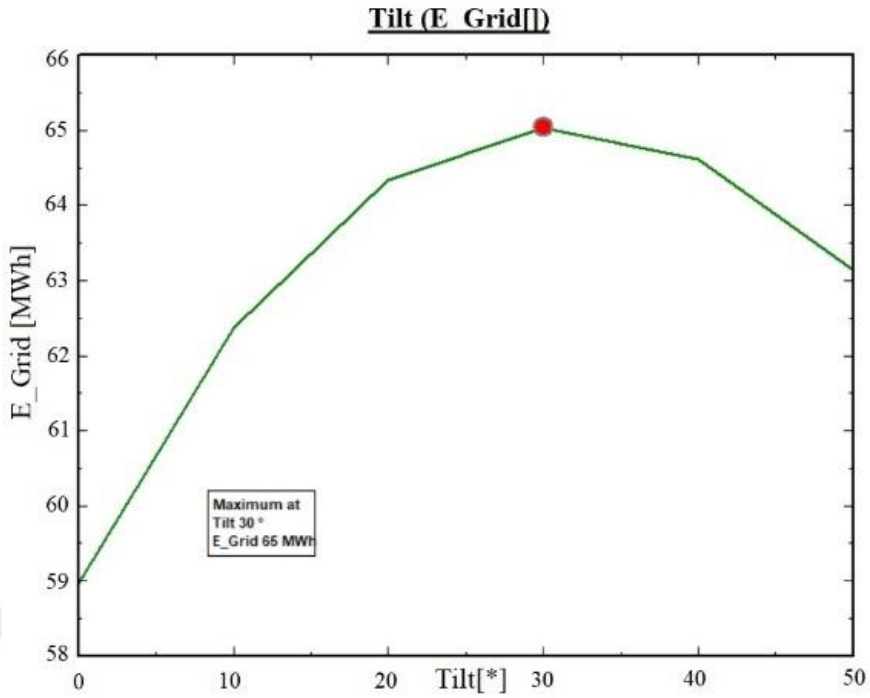

Figure 7.2. Tilt vs. E_grid

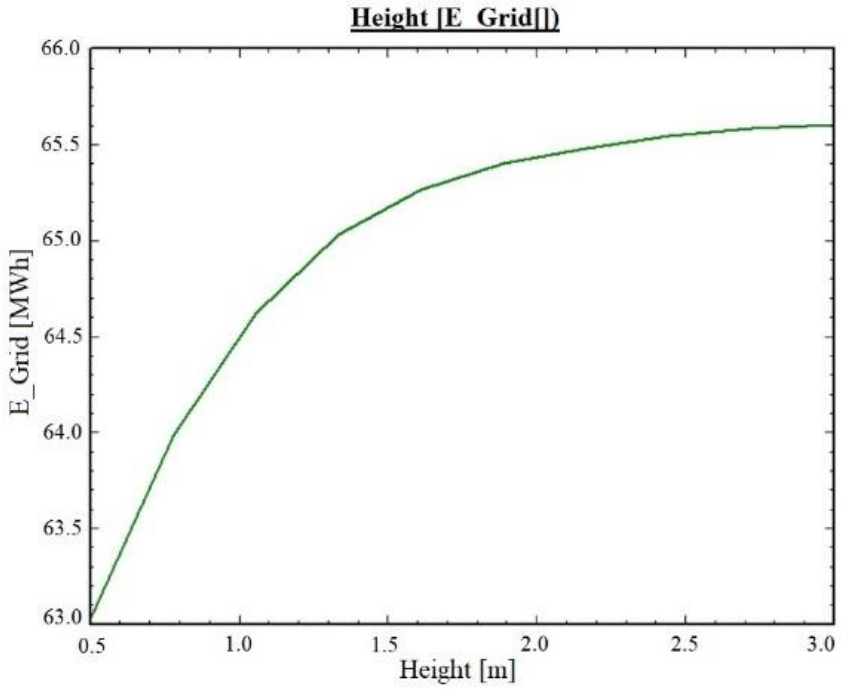

Figure 7.3. Elevation height vs. E_Grid

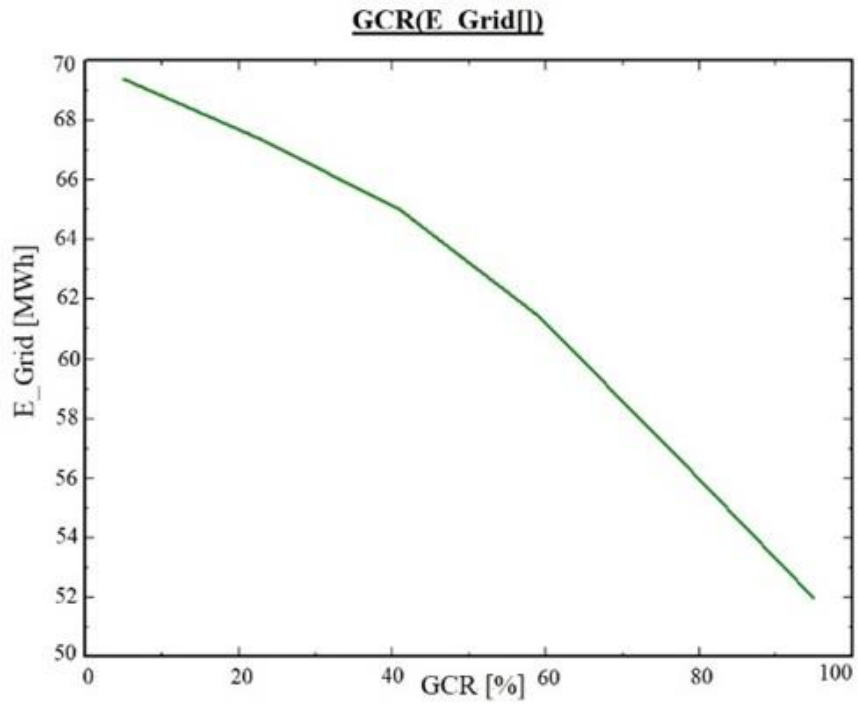

Figure 7.4. Ground coverage ratio vs. E_Grid

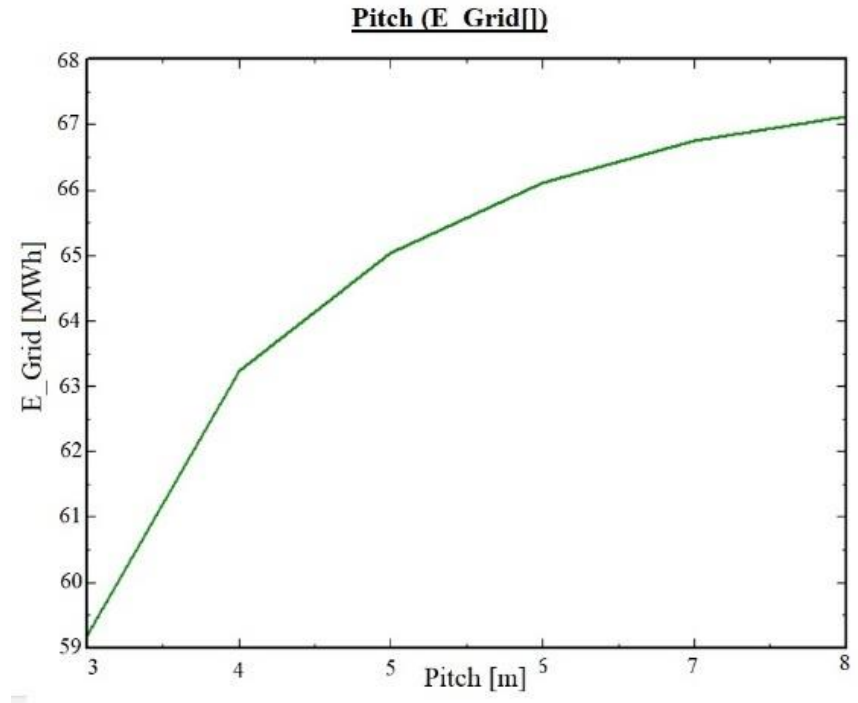

Figure 7.5. Pitch vs. E_grid

7.2 Simulation Results

The performance ratio (PR) is calculated by dividing the final PV system yield (Yf) by the reference yield (Yr). Figure 7.6. shows the PV performance ratio (PR). Our PV system's performance ratio value is relatively high because of the bifacial module gains. Figure 7.7. shows the normalized production and loss factors yielded annually.

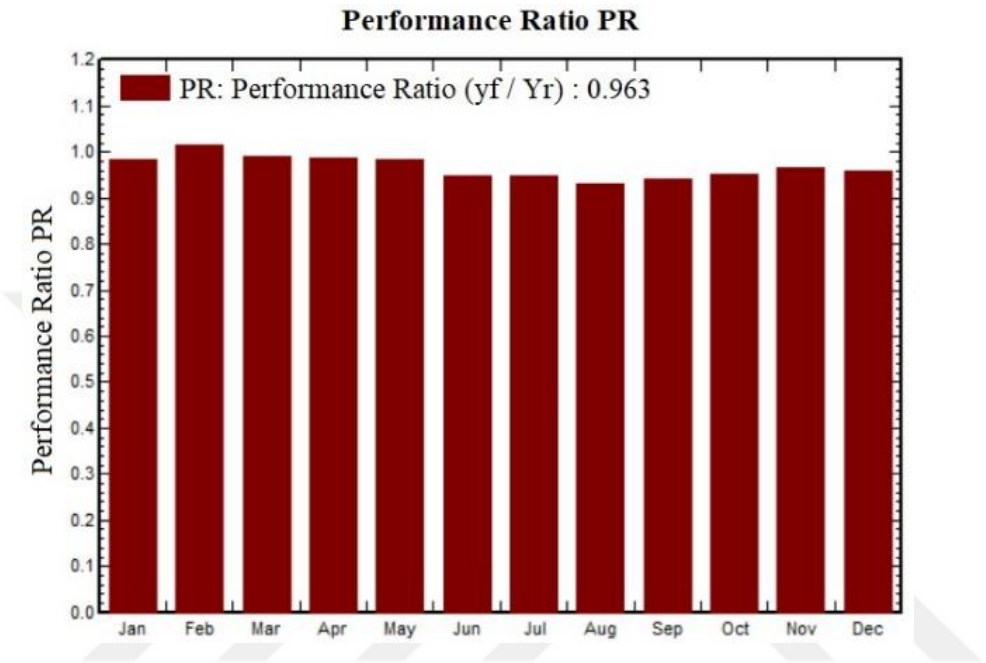

Figure 7.6. Performance ratio

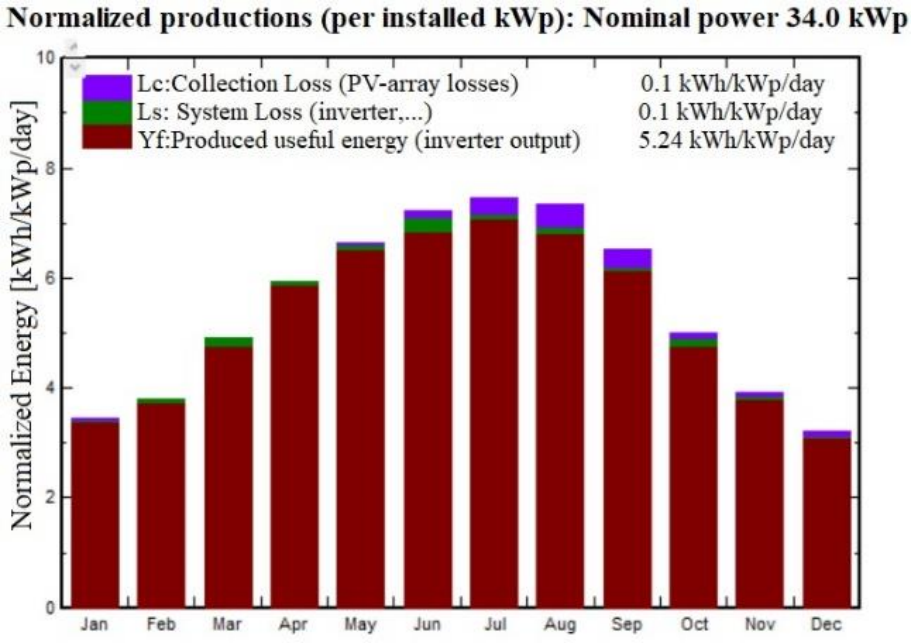

Figure 7.7 Normalized productions

The daily system output energy graph demonstrates how energy fed to the grid changes by months (see Figure 7.8.). Also, the incident irradiation distribution graphic tells us about changing incident irradiation in collector planes over the year in Figure 7.9. The bottom Figure 7.10. shows the system loss diagram. After subtracting all system losses, the final power fed to the grid is 65.0 MWh. The everyday Input/Output chart and system output power distribution are seen in Figure 7.11. and Figure 7.12., separately.

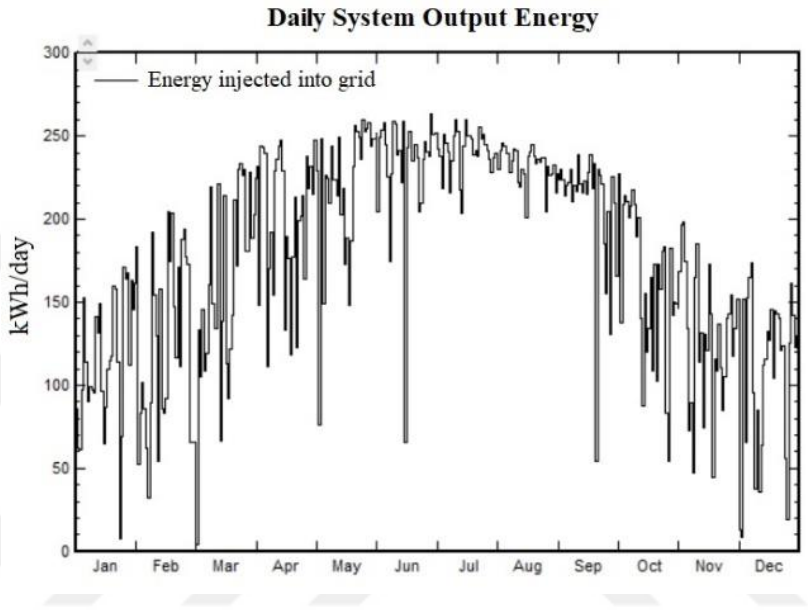

Figure 7.8. Daily system output energy

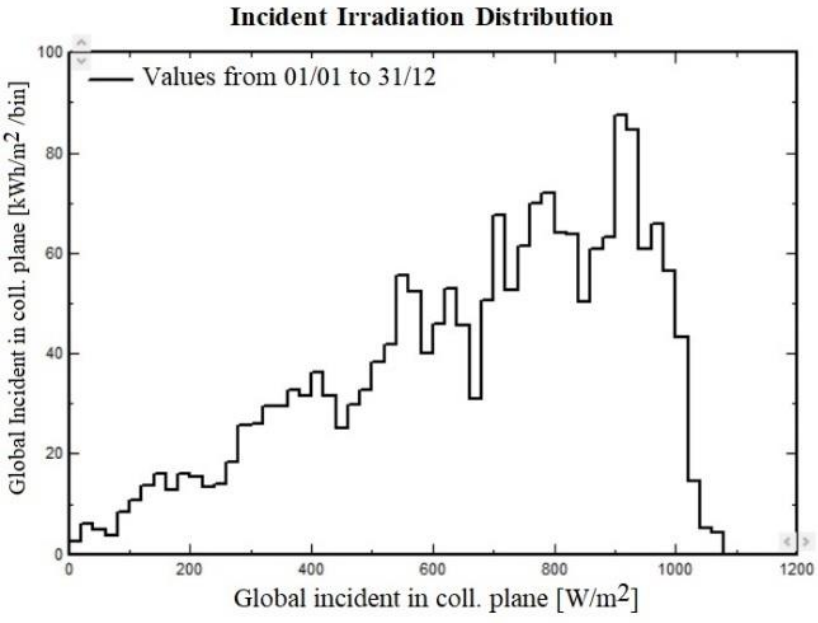

Figure 7.9. Incident irrigation distribution

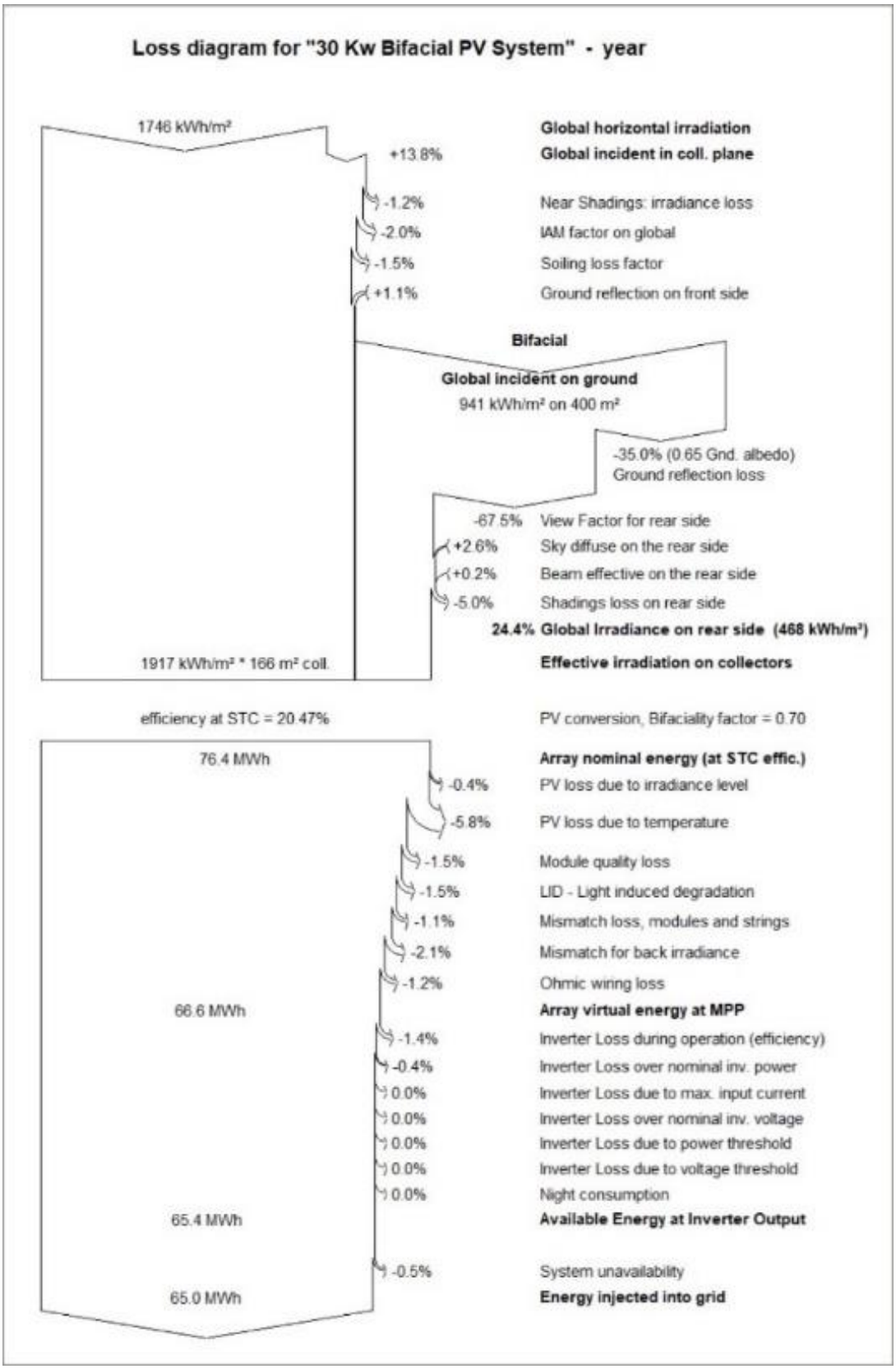

Figure 7.10. Loss diagram

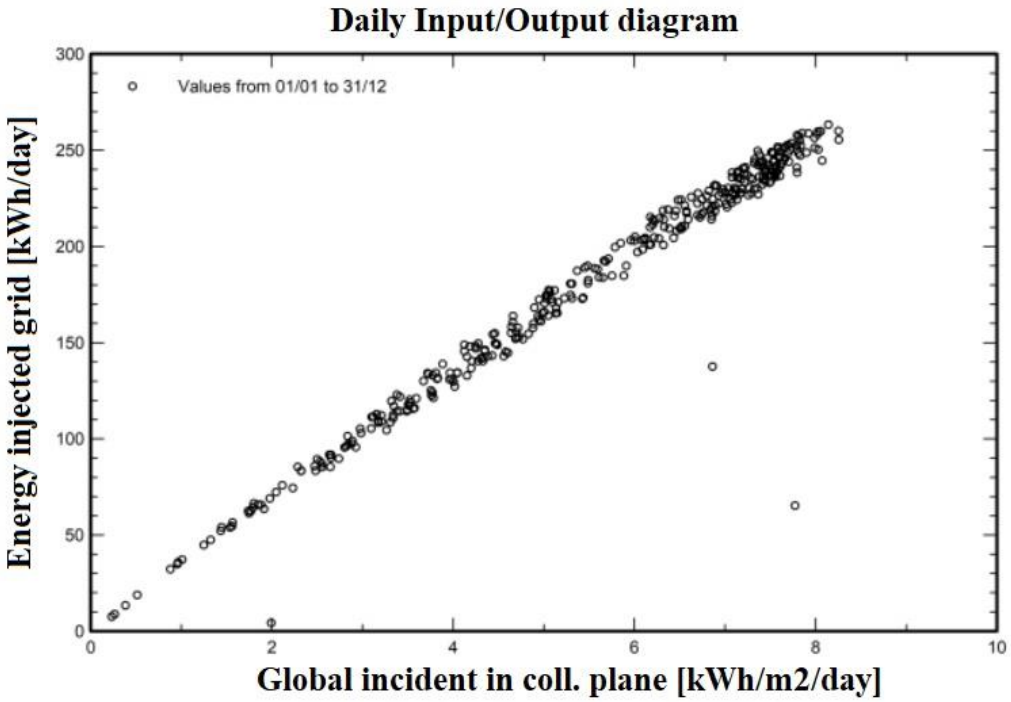

Figure 7.11. Daily Input / Output diagram

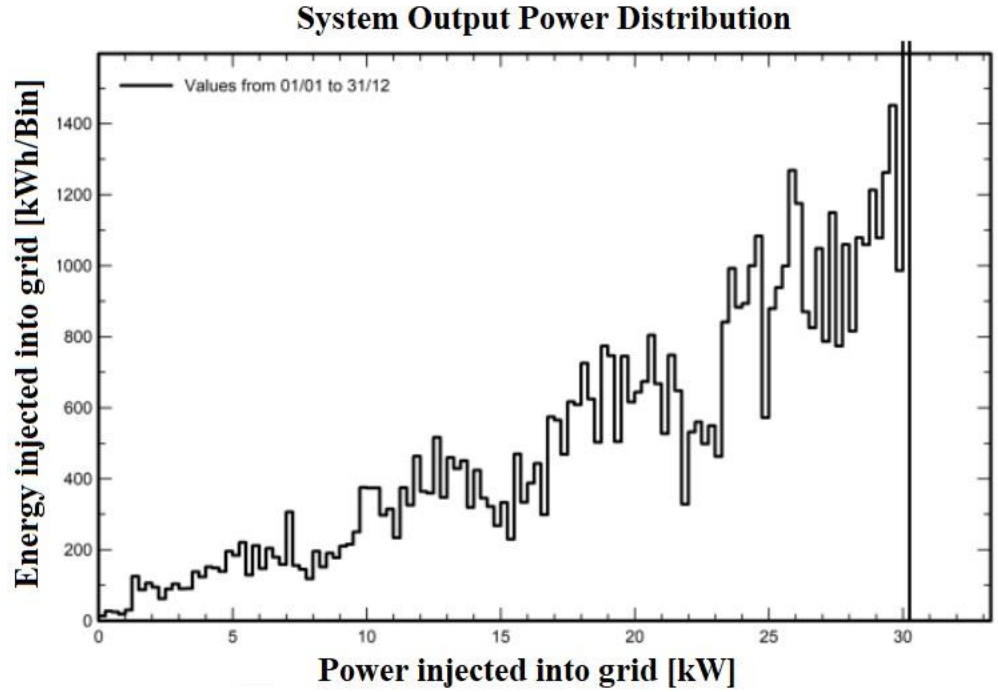

Figure 7.12. System Output Power Distribution

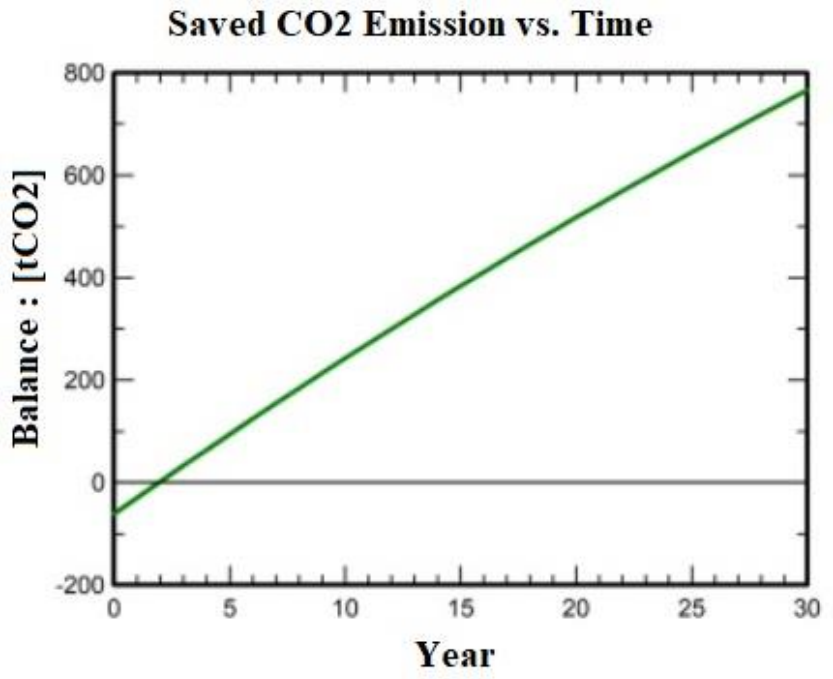

Figure 7.13 Saved CO_2 emission vs. time

A PV system modules, components, and other equipment cause some CO2 emissions in their first production. However, they do not emit CO2 throughout their operating life. And then, the gap will be closed within two or three years, and then a serious amount of CO2 emission will be prevented. (See Figure 7.13.)

7.3 Comparisons and Fundamental Results

Table 3 shows the comparisons and fundamental results for variables like irradiations, temperatures, system energies, and PR ratio. For our location, the yearly global irradiance on a horizontal plane is 1746.3 kWh/m^2. Annual energies per square meter of the global incident on the plane and effective global irradiance are 1987.2 kWh/m^2 and 1916.9 kWh/m^2, seperately. Based on that active irradiance, yearly AC energy fed to the grid and yearly DC energy generated from the PV array are 65 MWh and 66.30 MWh. A PV array's yearly mean yield is 20.10 percent, while the system's yearly mean yield is calculated to be 19.07 percent.

Table 3. Comparisons and fundamental results

Month	GlobHor kWh/m²	DiffHor kWh/m²	T_Amb °C	GlobInc kWh/m²	GlobEff kWh/m²	EArray Mwh	E_Grid Mwh	PR Ratio
January	68.2	31.68	6.64	106.5	102.4	3.611	3.561	0.984
February	77.2	39.65	8.25	103.5	99.8	3.617	3.566	1.014
March	125.6	61.22	11.57	149.6	144.2	5.170	5.030	0.989
April	164.8	74.58	15.60	178.1	171.5	6.068	5.985	0.988
May	209.4	77.53	21.08	206.0	198.4	6.979	6.882	0.983
June	229.4	72.96	25.84	216.4	208.8	7.261	6.971	0.948
July	240.1	64.83	29.46	231.3	223.4	7.566	7.462	0.949
August	215.0	59.06	29.16	227.5	219.9	7.296	7.194	0.930
September	163.9	50.07	23.85	195.7	189.0	6.339	6.253	0.940
October	115.7	45.96	18.37	155.2	150.0	5.170	5.015	0.951
November	76.9	33.11	12.66	117.7	113.5	3.924	3.868	0.967
December	59.9	24.61	8.06	99.8	96.0	3.297	3.250	0.958
Year	1746.3	635.26	17.60	1987.2	1916.9	66.299	65.038	0.963

7.4 Simulation Results and Analysis

Simulations on different albedo surfaces were performed to analyze the gain of the albedo effect in bifacial PV systems. The power and gain provided to the grid were computed using dark surfaces with a low albedo and bright surfaces with a high albedo. PVsyst simulation made closed the bifacial panel feature, and the power injected into the grid was just 56.4 MWh. **The reference surface with an albedo value of 0.65 underlined in table 3. was taken as a reference albedo point in the PVsyst base calculations. According to this albedo, the system injected 65.0 MWh of energy into the grid. It can be clearly from here that the 15.25% gain is obtained from the reference albedo value of 0.65.** The table shows that the higher the Albedo value, the higher the power supplied to the grid. The power gain corresponding to each albedo value was calculated as a percentage. As a result of the calculation, the gain of the PV system varies between 1% and 20% in average albedo values. The last calculation was made for white paint of the high-value albedo. The power injected into the grid is as much as 67.9 MWh, and the power gained is 20.39%. As you can see, the gain exceeds 20%. All the results obtained are shown in Table 4. with the title of typical albedo values of different kinds of surfaces and E_Grid and gain results.

As seen in Table 4, as the albedo value increases linearly towards 1, the gain of the bifacial system also increases linearly up to 20%. So, as a result, we can achieve a gain of 20% or more compared to a monofacial PV system.

Table 4. Typical albedo values of different kinds of surfaces and simulation results

Surface	Albedo	Albedo (Avg.)	E_Grid (MWh)	Gain (%)
Oceans	0.05 - 0.10	0.075	57.6	1.02
Asphalt	0.05 - 0.20	0.125	58.3	3.37
Corrugated roof	0.10 - 0.15	0.125	58.3	3.37
Trees	0.15 - 0.18	0.165	58.8	4.26
Red/Brown roof tiles	0.10 - 0.35	0.225	59.6	5.67
Colored paint	0.15 - 0.35	0.25	60.0	6.38
Gray portland cement concrete	0.20-0.30 (old)	0.25	60.0	6.38
Grass	0.25 - 0.30	0.275	60.3	6.91
Brick/Stone	0.20 - 0.40	0.30	60.6	7.44
Gray portland cement concrete	0.35-0.40 (new)	0.375	61.6	9.22
Ice	0.30 - 0.50	0.40	61.9	9.75
White portland cement concrete	0.40-0.60 (old)	0.50	63.2	12.06
Reference Surface	0.65 (ref. value)	0.65	65.0	15.25
White paint	0.50 - 0.90	0.70	65.6	16.31
Old snow	0.65 - 0.81	0.73	66.0	17.02
White portland cement concrete	0.70-0.80 (new)	0.75	66.2	17.38
Fresh Snow	0.81-0.88	0.845	67.3	19.33
White paint (high value)	0.90	0.90	67.9	20.39

Figure 7.14. White concrete

Figure 7.15. White paint

Figure 7.16. Snow

Figure 7.17. Soil-grass

The views of some surfaces with different albedo values are given in the white concrete in Figure. 7.14., white paint in Figure 7.15., snow in Figure 7.16., and soil-grass in Figure 7.17.

CHAPTER 8
CONCLUSIONS

Using PVsyst V7.2 simulation software, an analysis of the albedo effect in a 30-kW bifacial PV system with different ground surfaces was performed at the Caferbey, Salihli, Manisa, TURKEY, located at a latitude of 38.4772 N and longitude of 28.0972 E at an altitude of 126 meters. PVsyst simulations were made firstly by taking the reference albedo value of 0.65, the optimum significant value practically applicable in the solar fields. Horizontal global irradiation was found at 1746.3 kWh/m^2 ,and the performance ratio was about 96.3%. 65.0 MWh of energy was sent to the grid from the inverter output, with a specific power generation of 1913 kWh/kWp/year. Thus, the performance analysis was done using PVsyst software, which gave a normalized production of 5.24 kWh/kWp/day. For the reference 0.65 albedo value, the power supplied to the grid was 65.0 MWh. When the bifacial panel features were closed in the PVsyst simulation, the power supplied to the grid fell to 56.4 MWh. Thus, the gain was calculated at 15.25%. Despite using a fixed-mounted solar field, this high gain from the albedo effect alone could be considered quite good. Moreover, bifacial panel costs have decreased considerably, and the price gap between monofacial and bifacial modules have closed. An albedo value of 0.65 could be achieved using white concrete or white paint on the ground, as shown in Table 2.

Nowadays, solar PV areas occupy less space as the new technologies help more power gain by the panel module surface area. Financial gain from bifacial PV system production is much higher than the cost of covering the ground with a thin thickness of white concreting or white painting at a high albedo. In addition, the solar panels will be prevented from soiling loss. Covering the ground with white concrete may not be possible in all areas, such as agricultural lands. However, different solutions can be found that provide high albedo value without concreting the soil. The important thing is to see that bifacial panels have a very high potential in terms of gain and efficiency and to benefit from it as much as possible to lower an LCOE.

In today's world conditions, life has become more expensive. Therefore, the most efficient use of energy has become vital. After reducing module and system costs, obtaining electricity from the sun has become the cheapest electricity generation method. Research and tests have shown that bifacial panels will come to the fore with albedo gain and will offer more efficient electricity production for the future.

With the development of domestic production technologies, bifacial panels are now produced in Turkey. Nowadays, It has become possible to achieve high efficiency with lower cost in bifacial modules. As higher solar cell technologies are developed, the cost of bifacial solar modules will decrease further and they will become more common.

REFERENCES

Akcan, E., Kuncan, M., Minaz, MR. Modeling and Simulation of 30 kW Grid-Connected Photovoltaic System with PVsyst Software. *European Journal of Science and Technology* 2020; *18*: 248-261. DOI: 10.31590/ejosat.685909

Alnoosani, A., Oreijah, M., Alhazmi, MW., Samkari, Y., Faqeha, H. Design of 100MW Solar PV on-Grid Connected Power Plant Using (PVsyst) in Umm Al-Qura University. *International Journal of Science and Research (IJSR)* 2019; *8*(11):356-363

Alrashdan, MHS., AlFlahat, EN., Saeed, MO., Altahhan, HMK., Kreishan, SM. Modeling and Simulation of PV ON Grid System Producing 10kwh in Ma'an Development Area Using PVsyst Software. *Journal of Electrical and Electronics Engineering (IOSR-JEEE)* 2019;*14:*31-37. DOI: 10.9790/1676-1403033137.

Ashley, E. (2008, September / October). *Environmental and Cost Benefits of High Albedo Concrete.*Concrete in Focus, pp 54-55.

Ayadi, O., Jamra, M., Jaber, A., Ahmad, L., Alnaqep, M. An Experimental Comparison of Bifacial and Monofacial PV Modules. In: IREC 12th International Renewable Engineering Conference; 14-15 April 2021: *IEEE*, 20612812.

Borrull, M. (2019, 20 May). Performance Optimization of Bifacial Module PV Power Plants Based on Simulations and Measurements. *Master Thesis in Renewable Energy Systems.* Hamburg University of Applied Sciences.

Chiodetti, M., Dupeyrat, P., Lindsay, A., Binesti, D., Lutun, E., Radouane, K., Mousel, S. PV Bifacial Yield Simulation with a Variable Albedo Model. In: EU PVSEC 32nd European Photovoltaic Solar Energy Conference and Exhibition; 30 May - 3 June 2016: EU PVSEC Publishing, Munich, pp 1449-1455

Coakley. JA. Reflectance, Albedo Surface. In: Curry JA, Pyle, JA, editors. Encyclopedia of Atmospheric Sciences. Seattle, USA: Elsevier Publishing House, 2003. pp.1914-1923.

Concrete Pavement Research and Technology. (2002, June). *Albedo: A Measure of Pavement Surface Reflectance.* Number 3.05. Retrieved from http://www.pavement.com

Deege Solar (2022). *Bifacial Solar Panels: What Are They and How Do They Work?* Retrieved 1 March, 2022 from https://www.deegesolar.co.uk/bifacial_solar_panels/

Deline, C., Pelaez, SA., Marion, B., Sekulic, B., Stein, J. (2019, 3 December) Understanding Bifacial Photovoltaics Potential : Field Performance.NREL, National Renewable Energy Laboratory

Dittrich, T.(2018). *Material Concepts For Solar Cells.*World Scientific, pp. 3-43. https://doi.org/10.1142/97 81786344496_0001

Dobos, E. Albedo. *Encyclopedia of Soil Science* 2003; *120014334*: DOI: 10.1081/E-ESS 120014334

Duffie, JA., Beckman, WA. (2013). Solar Engineering of Thermal Process. *Solar Energy Laboratory University of Wisconsin-Madison.* John Wiley & Sons.

Duran, C. (2012, August 16). Bifacial Solar Cells: High-Efficiency Design, Characterization, Modules and Applications. *Konstanzer Online-Publikations-System (KOPS).* http://nbn-resolving.de/urn:nbn:de:bsz:352-205361

Erdil, A., Erbıyık, H. Renewable Energy Sources of Turkey and Assessment of Sustainability. In: 11th International Strategic Management Conference; 23-25 July 2015: Elsevier Publishing House, pp. 669-679

GSES International (2021). *Introduction to PVsyst: The Best Solar Design Software for 2021.* Retrieved 27 July, 2021, from https://www.gsesinternational.com/blog/introduction-to-pvsyst-the-best-solar-design-software-for-2021/

GTC. *Photovoltaic Solar Systems*. http://gtctrade.com/en/

Guerro-Perez, J., Benavente, IM., Berbel, JN. (2019,Fall). The Bifacial Year. *BITEC Results 4*. Soltec

Hidalgo C., (n.d.) *Bifacial PV Technology: Technical Considerations.* Retrieved from https://www.dnv.com/article/bifacial-pv-technology-technical-considerations-186095

Honsberg, C., Bowden, S. (n.d.). *Solar Cell Efficiency.* Retrieved from https://www.pveducation.org/pvcdrom/solar-cell-operation/solar-cell-efficiency

International Energy Agency. (2021). *Bifacial Photovoltaic Modules and Systems: Experience and Results from International Research and Pilot Applications.* Report IEA-PVPS T13-14:2021

IRENA, International Renewable Energy Agency. *Renewable Energy Sources.* Retrieved from https://www.irena.org/solar

İzgi, E., Özcan, Ö. (2020, August 06) Comparative Performance Analysis of Grid-Connected Photovoltaic Roof System. *KSU J Eng Sci, 23(3), 2020.*

Kopecek, R., Libal, J. Bifacial Photovoltaics 2021: Status, Opportunities, and Challenges. *Energies 2021;14*: 1-16. DOI:10.3390/EN14082076.

Kotak, Y., Gul, MS., Muneer, T., Ivanova, SM. Investigating the Impact of Ground Albedo on the Performance of PV Systems. In: CIBSE Technical Symposium; 16-17 April 2015: CIBSE Publishing, London: pp. 1-16

Langels, H., Gannedahl F.(2018, June). *BiFacial PV Systems; A technological and financial comparison between BiFacial and standard PV panels.* Uppsala Universitet

Levinson, R., Akbari, H. (2001, December). Effects of Composition and Exposure On the Solar Reflectance of Portland Cement Concrete. *Environmental Energy Technologies Division Lawrence Berkeley National Laboratory University of California*

LG (2017). *Bifacial Design Guide*. https://www.lg.com/global/business/download/resources/solar/Bifacial_design_guide_Full_ver.pdf

Lusson, N. (2020). *Bifacial modules: The challenges and advantages*. Retrieved August 19, 2020, from https://www.pv-magazine.com/2020/08/19/bifacial-modules-the-challenges-and-advantages/

Mirhosseini, N., Mirani MR., Miri, T. (2018, February). *The Science of Renewable Energy on Global Warming: a Review of Greenhouse Gases Emission*. 4TH National Conference of Iran Chemistry, Chemical Engineering, and Nano.

NRDC (2018). *Renewable Energy: The Clean Facts.* Retrieved 15 June, 2018, from https://www.nrdc.org/stories/renewable-energy-clean-facts

Ns Energy (2019). *Karapınar Solar Power Project*. Retrieved December, 2019, from https://www.nsenergybusiness.com/projects/karapinar-solar-power-project/

Nygren, A., Sundström, E. (2021, 06 November). *Modeling Bifacial Photovoltaic Systems*. School of Business, Society and Engineering. Malardalen University Sweden. .

Ooshaksaraei, P., Sopian, K., Zulkifli, R., Alghoul, MA., Zaihidi, SH. Characterization of a Bifacial Photovoltaic Panel Integrated with External Diffuse and Semimirror Type Reflectors. *International Journal of Photoenergy* 2013; *1*:1-7. DOI: 10.1155/2013/465837.

Rekioua, D., Matagne, E. (2012) Optimization of Photovoltaic Power Systems. Modelization, Simulation, and Control. Springer Science&Business Media.

Renewables now(2022). *Turkey's Karapınar PV Plant to Be Fully Operational by End 2022 -report.* Retrieved April 19, 2022, from https://renewablesnow.com/news/turkeys-karapinar-pv-plant-to-be-fully-operatio nal-by-end-2022-report-781406/

Saive, R., Augusto, A., Atwater, HA., Bowden, SG., Russell, TCR. The Influence of Spectral Albedo on Bifacial Solar Cells: A Theoretical and Experimental Study. *IEEE Journal of Photovoltaics* 2017; *7*(6): 1 – 8. DOI: 10.1109/JPHOTOV.2017.2756068

Sanchez-Ortiz, H., Meza, C., Dittmann, S., Gottschalg, R. (2020, November) The Effect of Clearance Height, Albedo, Tilt and Azimuth Angle in Bifacial PV Energy Estimation Using Different Existing Algorithms. *Proceedings of the III Ibero-American Conference on Smart Cities (ICSC-2020).*

Satpathy, R. (n.d.). *Additional Energy yield using Bifacial Solar PV Modules & dependency on Albedo.* Jackson, Empowering People.

Sreenath, S., Sudhakar, K., Yusop, AF. Performance Assessment of Conceptual Bifacial Solar PV System in Varying Albedo Conditions. In: IPCME 2021 IOP Conf. Series: Materials Science and Engineering; 18-23 July 2021:*IOP Publishing*, pp. 1-9.

Toplicic-Curcic, AT., Ristic, N., Grdic, D., Grdic, Z. (2016, January). White Cement Concrete an Element of Sustainable Building. *Article in Zbornik radova Građevinskog fakulteta.* DOI: 10.14415/konferencijaGFS2016.041

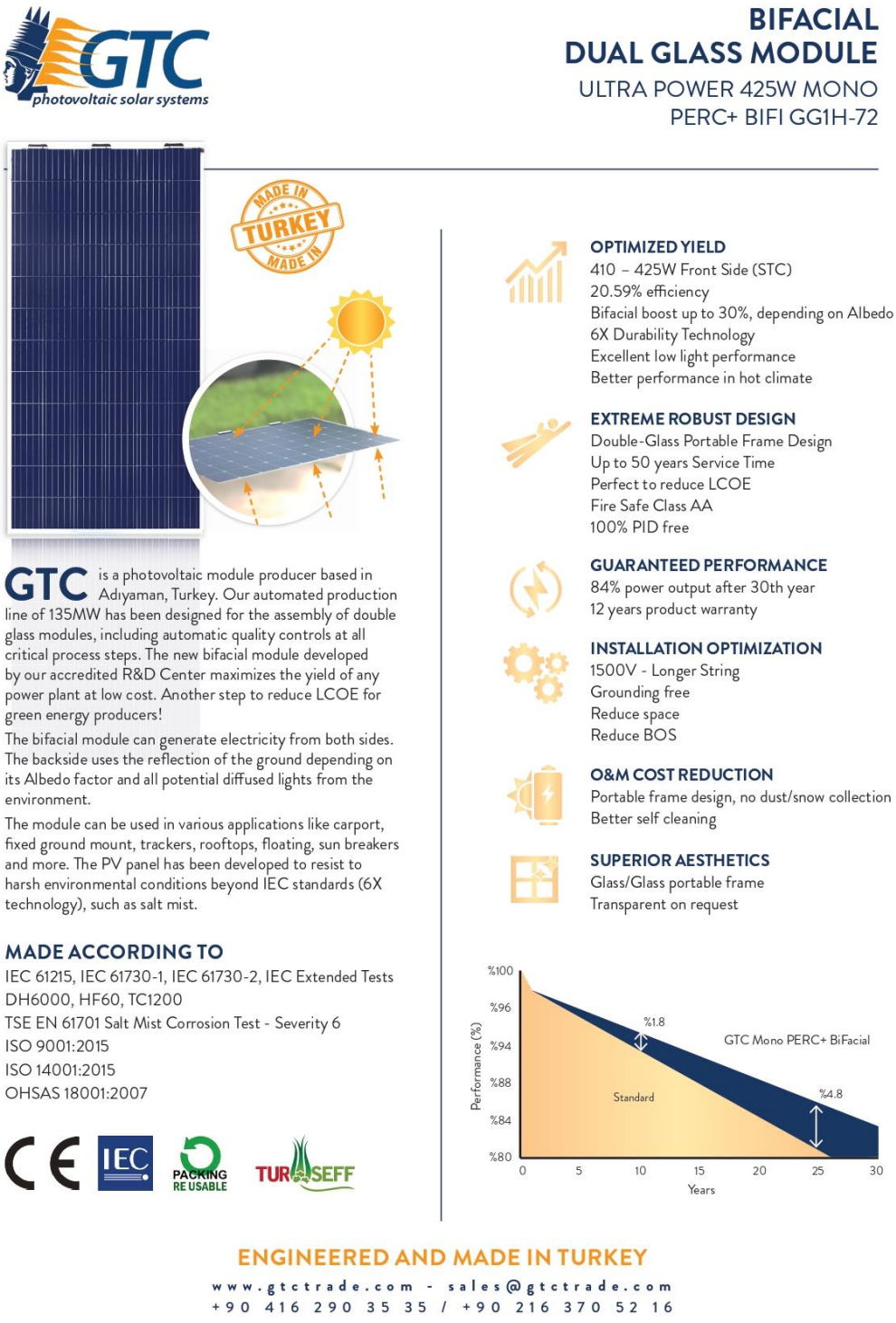

Figure A1.1. GTC Bifacial dual glass module datasheet -1 (From gtctrade.com)

GTC photovoltaic solar systems

BIFACIAL DUAL GLASS MODULE

ULTRA POWER 425W MONO PERC+ BIFI GG1H-72

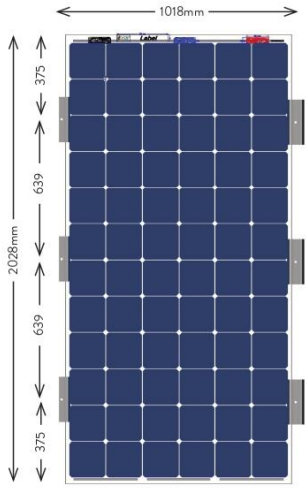

ELECTRICAL PERFORMANCE

Max. Power P_{max} (W)	410	415	420	425
Max. Power Voltage V_{MPP} (V)	40.65	40.74	40.82	41.08
Max. Power Current I_{MPP} (A)	10.09	10.19	10.29	10.35
Open-Circuit Voltage V_{oc} (V)	48.80	48.95	49.10	49.45
Short-Circuit Current I_{sc} (A)	10.29	10.60	10.90	11.15
Performance n_m (%)	19.80	20.10	20.34	20.59

Standard Test Conditions (STC); 1000 W/m2, AM1.5, 25 °C, Power Tolerance (W) +/- 3%

BOOST FROM THE BACKSIDE

+7%	Power (W)	439	444	449	455
	Performance (%)	21.20	21.51	21.77	22.03
+15%	Power (W)	472	477	483	489
	Performance (%)	22.84	23.12	23.40	23.77

Bifaciality depends on Albedo

ELECTRICAL PARAMETERS AT NOMINAL OPERATING CELL TEMPERATURE (NOCT)

Power Output P_{MAX} (W)	305	309	312	316
Max. Power Voltage V_{MMP} (V)	37.65	37.77	37.88	38.00
Max. Power Current I_{MMP} (A)	8.10	8.17	8.24	8.32
Open-Circuit Voltage V_{oc} (V)	44.90	45.30	45.70	46.00
Short-Circuit Current I_{sc} (A)	8.65	8.76	8.86	8.94

NOCT: open-circuit module operation temperature at 800W/m2 irradiance, 20°C ambient temperature, 1m/s wind speed

I-V CURVE (PV MODULE 425W)

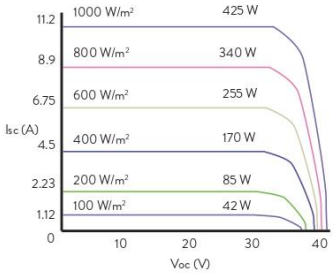

P-V CURVE (PV MODULE 425W)

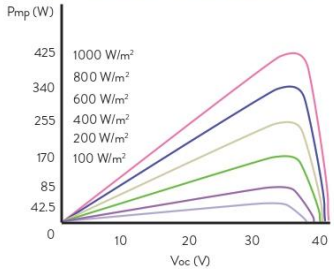

OPERATING CONDITIONS

Operating Temperature	-40°C/+85°C
Max. System Voltage	1500V
Max. Series Fuse Rating	20A
Wind Load	2400 Pa
Snow Load	5400 Pa

TEMP. CHARACTERISTICS

Temp. coefficient P_{MAX}	-0.38%/K
Temp. coefficient V_{OC}	-0.29%/K
Temp. coefficient I_{SC}	0.04%/K
Nominal Operating Temperature (NOCT)	46°C

MATERIAL SPECIFICATION

Front Cover	2.5mm ARC Low Iron Tempered Solar Glass
Cell Type	Bifacial Mono PERC
Cell Matrix	72 Cells (6 x 12)
Lamination material	EVA
Back Glass	2.5mm ARC Low Iron Tempered Solar Glass
Junction Box	IP67 rated, 1500V Compatible, 3 Diodes
Cables and connectors	DC Cable 4 mm² MC4 compatible, 1500 V Cable length 15cm male - 40cm female
Frame	Portable Frame
Module Dimensions	2028 mm x 1018 mm x 6 mm (without J-box)
Module Weight	29.9 kg
Module Per Box	30
Box per Truck	24

ENGINEERED AND MADE IN TURKEY

www.gtctrade.com - sales@gtctrade.com

+90 416 290 35 35 / +90 216 370 52 16

Figure A1.2. GTC Bifacial dual glass module datasheet- 2 (From gtctrade.com)

GTC BIFACIAL SOLAR PANEL SPECIFICATIONS

- Panels with a local content rate of more than 50%
- Floaters with a local content rate of more than 50%
- Local panel technology
- Local floater technology
- Turnkey
- Electricity Generation Guaranteed
- Highest level of electricity generation per m2
- Fire Protection
- Performance Guaranteed 84% in 30 Years
- Least maintenance
- Least electricity cost
- Not prevent the sunlight from reaching the sea
- Bifacial electricity generation through the sunlight reflected on the water
- 7% plus electricity generation per m2 at minimum compared to HDPE standard systems.
- Resistant to waves, wind and punctures
- Moisture resistant, double-glass solar panels with 6 times more endurance
- Salt mist corrosion endurance at the 6th level of severity
- We contribute to the sustainability of the ecosystem, the maximum system lifecycle and cheapest electricity through non-combustible, non-flammable solar panels.
- 7% plus electricity generation on ground at minimum
- 10% plus electricity generation at minimum in case of a breaker installed on ground
- High efficiency generation even during a storm
- 10% plus electricity generation at minimum
- Ultralight construction
- Resistance to wind load of 155 km/h according to the SAP 2000 report.
- 5% plus electricity generation per m2 at minimum compared to standard solar panels.

- Solar panels with Class AA fire protection fire shields.
- Class B1 fire protection
- Elegant look for your building
- Sound and heat insulation
- Zero energy, environmentally friendly buildings
- An elegant look with specially designed, double-glass solar panels
- Watertightness
- Highest level of electricity generation per m2
- Charging station for vehicles
- Protects vehicle from the rain and sun
- Environmentally friendly carparks
- Light and thin glassed solar panels
- Roof-tile shaped solar panels
- High performance solar panels with micro-inverters
- Class AA fire protection
- Maintenance-free solar energy systems as durable as your building.
- Special, light and thin glassed solar panels
- Sunlight as much as you need
- Greenhouses with lower carbon emissions thanks to specially designed solar panels usable as greenhouse glasses
- Maximum Front Side Output (STC) Wide Power Range 22.15% average Panel Efficiency Extra Power production up to 30% 6x Resistance Technology
- Perfect performance at low light Much better performance in hot climates
- Portable Frame design, no dust/snow accumulated less rate of contamination
- Double-Glass Portable Frame Design Up to 50 years Service Time Perfect to reduce LCOE Fire Safe Class AA 100% PID free
- Panels that have passed the age-temperature test for 6000 hours, moisture-freeze test and thermal cycle test, and that is registered with a 6 times endurance performance (performance guarantee: 84% in 30 years) under the IEC 61215 standard.
- Fire protection class: AA according to the UL 1703 standard and, B-S1,d0 according to the TS EN 13501-1 standard.
- Superior mechanical strength against snow and wind load.

The highlighted features of our bifacial solar panels:

- Our bifacial solar panels are of glass-glass panels that have passed 6X tests under the IEC 6215 standard proving that the yield loss would be only 16% in 30 years.

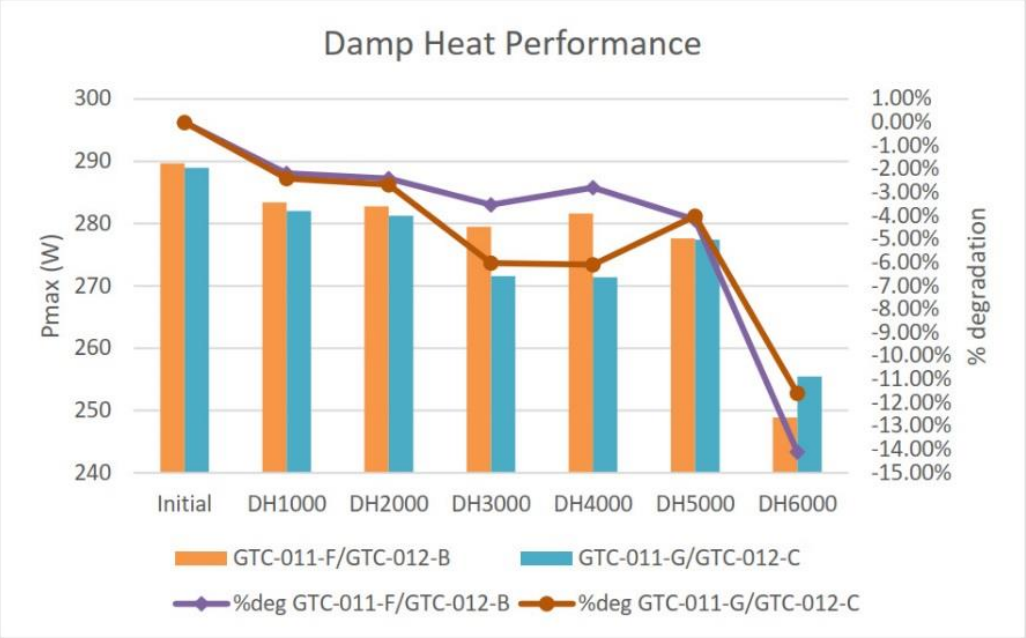

Figure A1.3. Damp heat performance (From gtctrade.com)

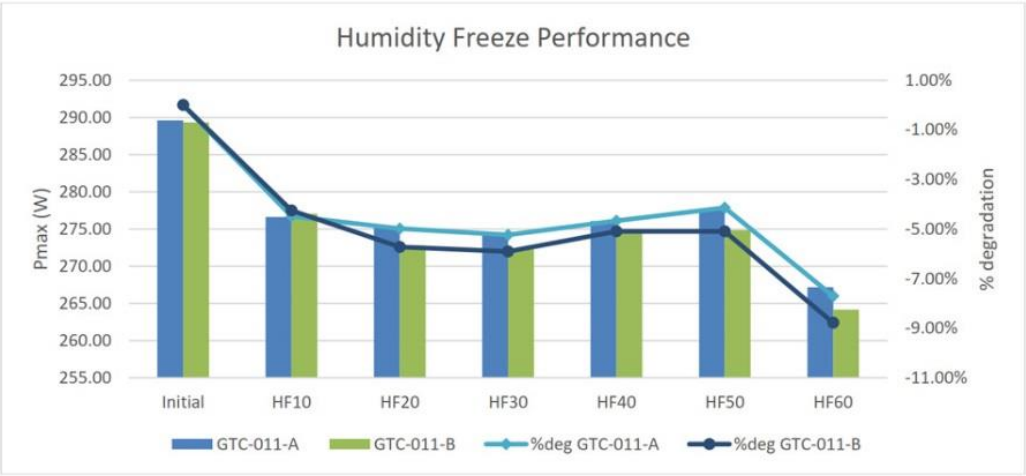

Figure A1.4. Humidity freeze performance (From gtctrade.com)

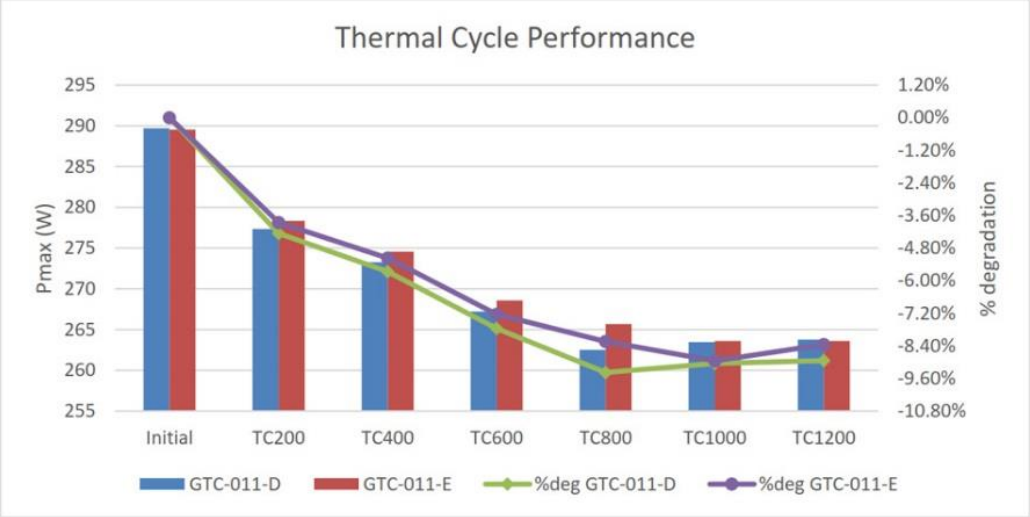

Figure A1.5. Thermal cycle performance (From m gtctrade.com)

GTC Bifacial Solar Cell's 6X Technology

6X includes extended endurance testing performed by recognized laboratories in accordance with IEC module certification criteria. This controls how the power of a solar panel degrades over time. For module makers, the criteria outlined in the fundamental standards IEC 61215 and IEC 61730 would apply to a 1000-hour age-temperature test (DH1000), a 200-cycle thermal cycle test (TC200), and a 10-cycle moisture-freeze test (HF10) as 1X at 80 degrees Celsius and 80% relative humidity. These are the approval tests, however they don't reflect the aging of the panel.

The 6X tests are a variation of the certification testing that is six times longer and includes the following tests: a 6000-hour age-temperature test (DH6000), a 200-cycle thermal cycle test (TC1200), and a 60-cycle moisture-freeze test (HF60).

The conventional frame modules fail to pass more than 3X aging process tests, and the majority of them do not even pass a 2X test. The 3000 hour outside tests, they assert, are not aging process testing. They are, however, sold with a 25-year performance warranty. Our performance guarantee is an 84 percent capacity in 30 years, according to our 6X aging process test findings. Our products provide the lowest level of electricity cost in the world, with a power reduction promise of not more than 16 percent for 30 years. The salt mist endurance test at the 6th degree of severity was also passed by our solar panels.

Figure A1.6. Tasarruf Enerji – Elazığ. Project Type: Bifacial Fields

(From gtctrade.com)

Figure A1.7. İstinye Park SPP- İzmir BIPV (Building - Integrated PV)

(From gtctrade.com)

Figure A1.8. Balcony Project – İstanbul (From gtctrade.com)

Figure A1.9. Greenhouse (From gtctrade.com)

Figure A1.10. Escom Power SPP – Niğde. Project Type: Bifacial Roof (From gtctrade.com)

Figure A1.11. TAV Muğla Airport SPP. Project Type: Bifacial Carpark (From gtctrade.com)

Figure A1.12. Floating SPP – İstanbul (From gtctrade.com)

Figure A1.13. NUÇA and Doğa SPP (From gtctrade.com)

Figure A1.14. DBE – Derbent – Konya. Project Type: Bifacial Tracker (From gtctrade.com)

APPENDIX 2 – A Brief Overview of Renewable Energy

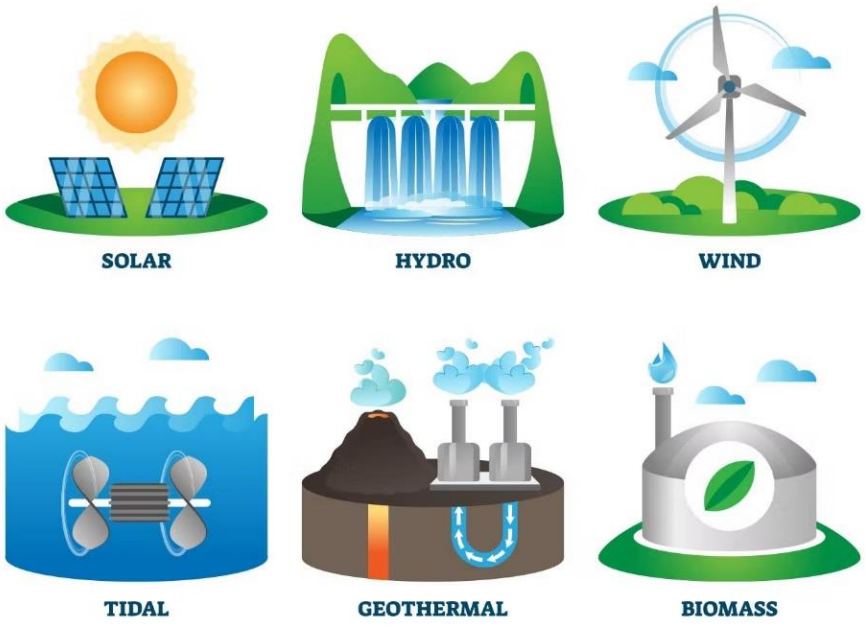

Figure A2.1. Types of renewable energy sources (From inspirecleanenergy.com)

What Is Renewable Energy?

Renewable energy, often known as clean energy, is produced at constantly replenished from natural processes (See Figure A2.1.). Even though wind and sunlight affected by time and weather, they continue to shine and blow.

Even though harnessing nature is often considered a new technology, it has been used for years for warmth, lightining, transportation and other reasons. Boats sail the seas on wind power ,and grain mills grind grain on wind power. The sun has provided heat during the day, and fires have been lighted into the evening due to the daytime warmth. As people used dirty energy sources more and more during the last 500 years, such as coal and hydraulic fracking gas, pollution increased.

In the world, renewable energy accounts for more than one-fourth of the country's electricity generation, thanks to more innovative and less expensive methods of capturing and storing solar and wind energy. Increasing amounts of renewable energy are becoming available at all scales, from PV systems on homes that sell electricity to the grid to huge offshore wind plants. Several remote villages rely totally on renewable energy for heating and lighting.

A key priority of the Turkish government, in addition to boosting renewable energy generation, is to upgrade the country's power system, making it more efficient, secure, and well-connected. The world all renewable energy installed capacity trends can be seen in Figure A2.3.

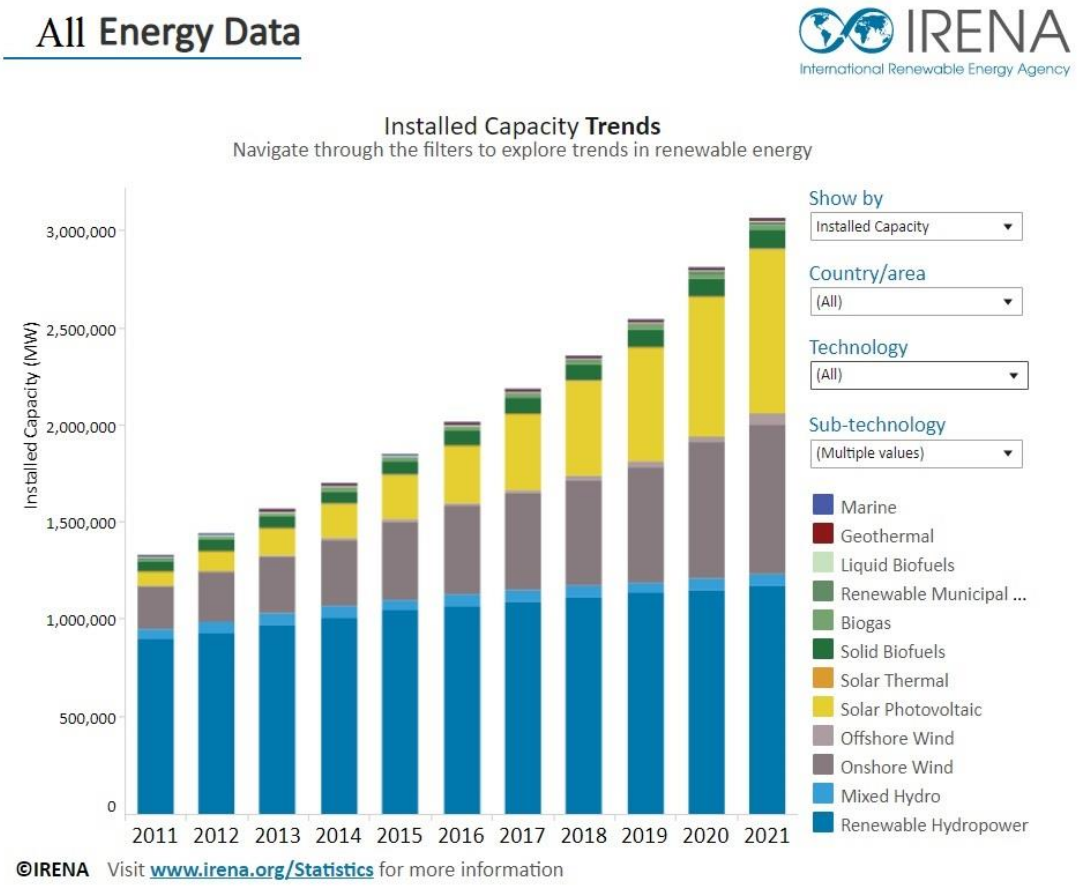

Figure A2.2. Global trends in renewable energy installed capacity (From IRENA)

Dirty energy:

Nonrenewable or "dirty" energy sources include fossil fuels such as gas, coal, and oil. Nonrenewable energy sources have finite quantities and replenishment takes a long time. When we pump gas at the station, we consume a finite resource derived from crude oil that has been there since earliest times.

Nonrenewable energy sources are also more abundant in several nations than others due to their geographic location. Sunlight and wind, however, are available in every country. In addition to strengthening national security, nonrenewable energy can be

prioritised because it will reduce a country's import-export dependency on fossil-fuel-rich countries.

Several nonrenewable energy sources have the potential to harm the environment as well as human health. Oil extraction, for instance, may necessitate opencast-mining Canada's north forest, fracking technologies may create water pollution, earthquakes and coal-fired power stations damage the atmosphere. On top of that, all of these actions occur to the cause of global warming.

RENEWABLE ENERGY SOURCES TYPES

Solar Energy:

Since thousands of years ago, humans have used solar energy to dry food, stay hot, and grow grains. Under to the Laboratory of National Renewable Energy, in one hour, the sun emits more energy than everyone on Earth uses in a year. We now use the sun's beams for a various purposes, including heating houses and businesses, heating water, and powering electronics.

The photovoltaic or solar cell is made of silicon or similar material and turns sun-light into energy directly. Solar distributed energy systems provide electricity to households and businesses on a local scale, either through roof PV system modules or group projects that power entire district. The energy provided by solar farms, which use mirrors to track sunlight onto thousands of panels, could power thousands of homes. Floating solar farms, known as "photovoltaics," are an environmentally friendly way to utilize wastewater facilities and bodies of water.

Most solar panels have a little environmental impact other than during the manufacturing process if installed correctly. Solar energy systems emit virtually no air pollutants or greenhouse gases. World Solar Energy installed capacity trends can be seen in Figure A2.3.

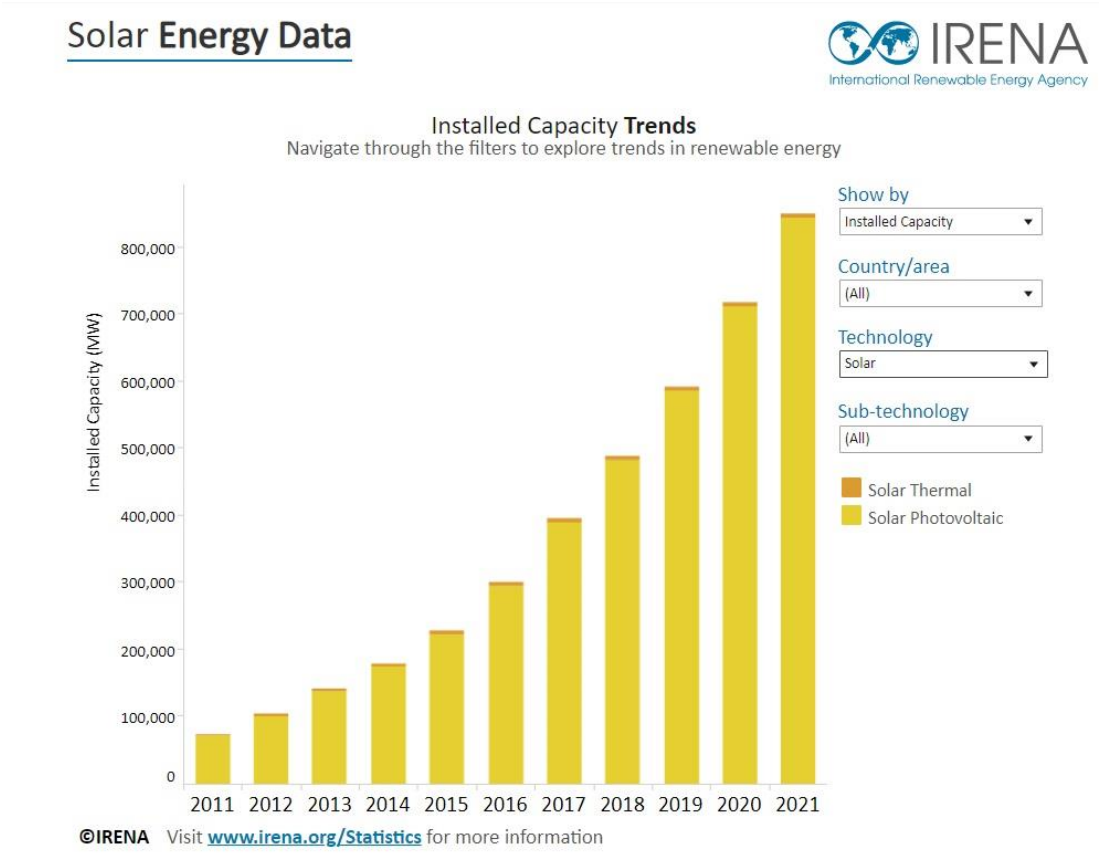

Figure A2.3. Global trends in solar energy installed capacity (From IRENA)

Wind Energy:

Windmills of the past are no longer in use. The world stands at attention today with turbines the height of buildings and a diameter comparable to the diameter of turbines. The turbine blades are rotated by wind energy, which feeds a wind turbine generator and creates electricity.

The wind has become the second-cheapest energy source in many countries like Turkey, making up over 11 % of total production. Turbines may be installed anywhere with strong wind speeds, including hilltops and broad plains, and offshore in the open ocean. World wind energy installed capacity trends can be seen in Figure A2.4.

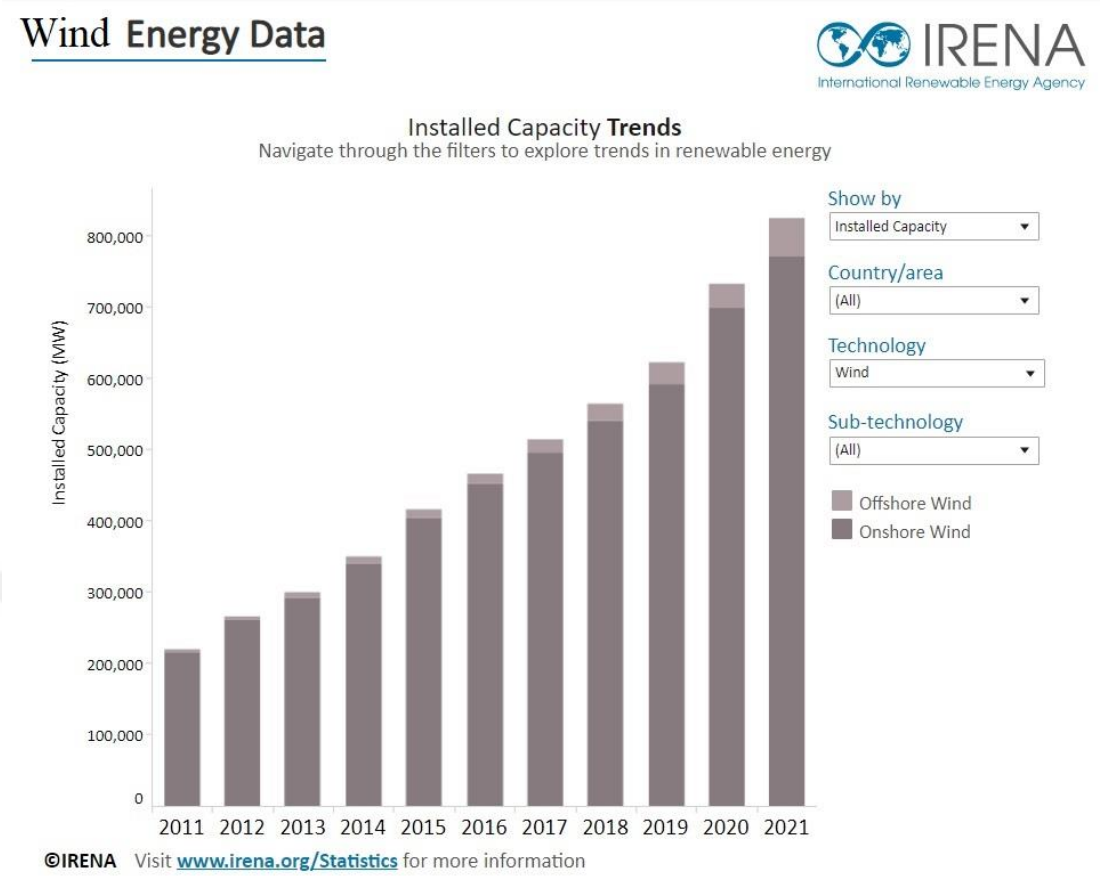

Figure A2.4. Global wind energy installed capacity trends (From IRENA)

Other Preferences For Energy Sources

Hydroelectric Power:

Currently, hydroelectric power is the most common renewable energy source for electricity. However, wind energy is likely to close it shortly. Using water as a power source, hydroelectric power generates electricity by spinning generator blades powered by fast-moving water - typically in a large river or rapidly falling water from a high-peak point. Large-scale hydroelectric power plants, sometimes known as mega-dams, are frequently considered nonrenewable energy sources domestically and globally. Mega-dams redirect and disrupt natural flows, limiting access for wildlife and humans reliant on rivers. Small hydroelectric facilities (with an installed capacity of fewer than 40 megawatts) cause less environmental impact since they divert just a fraction of the flow. World hydropower energy installed capacity trends can be seen in Figure A2.5.

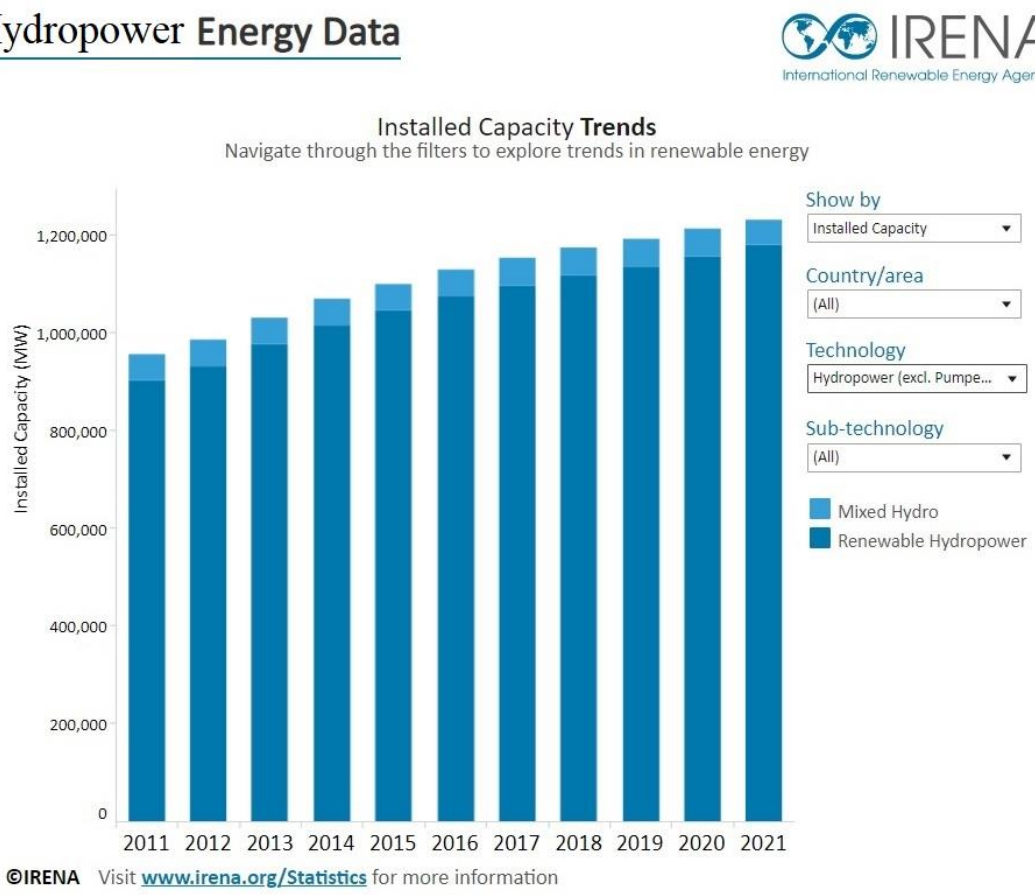

Figure A2.5. The global trends in hydropower installed capacity (From IRENA)

Biomass Energy:

Plants and animals produce biomass organic material in the form of trees, grains, and scrap wood. Chemical energy is released as heat when biomass is fired, which can be utilized to power a steam turbine to generate electricity. For energy generation, many people mistakenly believe that biomass is a cleaner, renewable fuel and a better alternative source of energy than other fossil fuels and coal. However, recent studies demonstrate that many types of biomass, especially those derived from forest lands, emit more carbon than fossil fuels. It is also seen in detrimental ecological repercussions for biodiversity. However, given the right circumstances, some types of biomass energy might be a low-carbon option. Sawdust and chips from sawmills, for example, may be used as a low-carbon energy source instead of decomposing and releasing carbon. World bioenergy installed capacity trends can be seen in Figure A2.5.

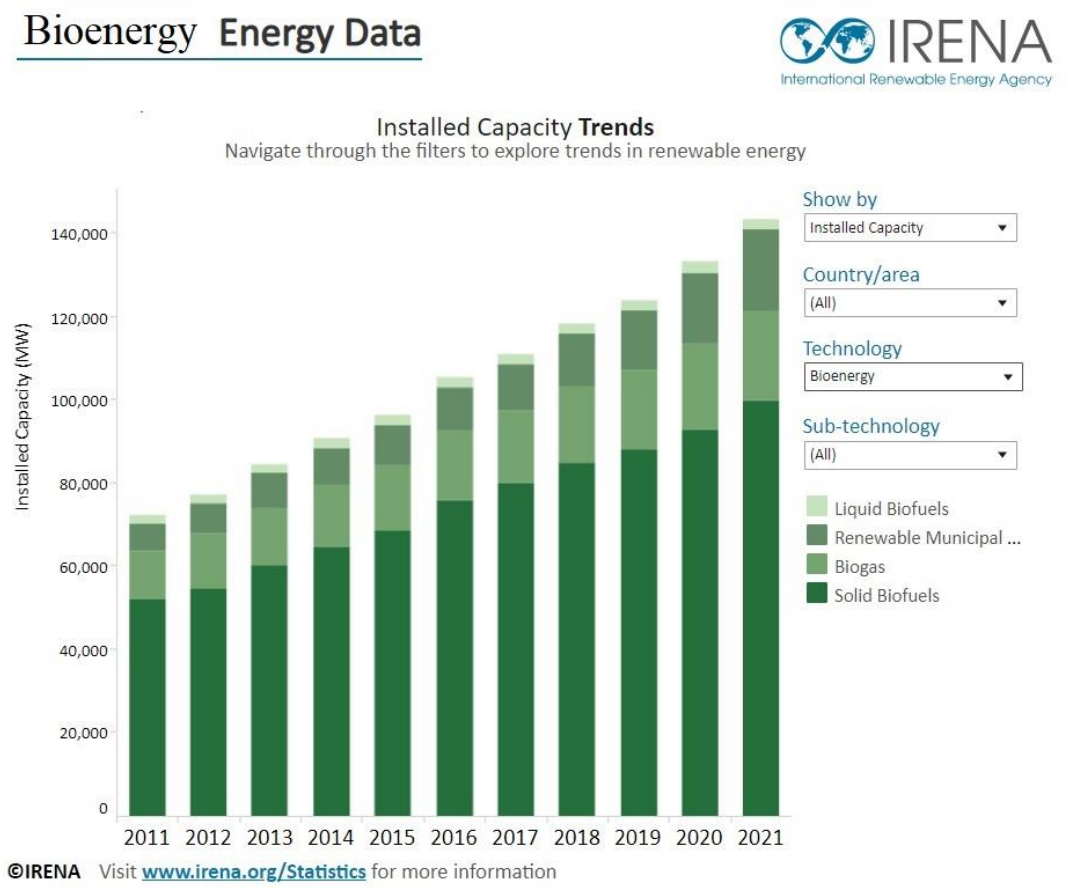

Figure A2.6. Global bioenergy installed capacity trends (From IRENA)

Geothermal Energy:

Geothermal energy is an environmentally renewable energy source because heat is always produced inside the earth. Because of the progressive degradation of radioactive particles in rocks in the earth's core, its core is nearly the same temperature as the sun's surface. Through drilling deep wells, very hot underground water can be brought to the surface to create hydrothermal resources that can be pumped to the surface and used as a source of electricity. Typically, geothermal plants emit low level emissions when their steam and water are pumped back into the reservoir. Geothermal plants can be constructed without underground reservoirs; however, there is fear that such facilities can trigger earthquakes in the geologically active places. Geothermal energy installed capacity trends can be seen in Figure A2.5.

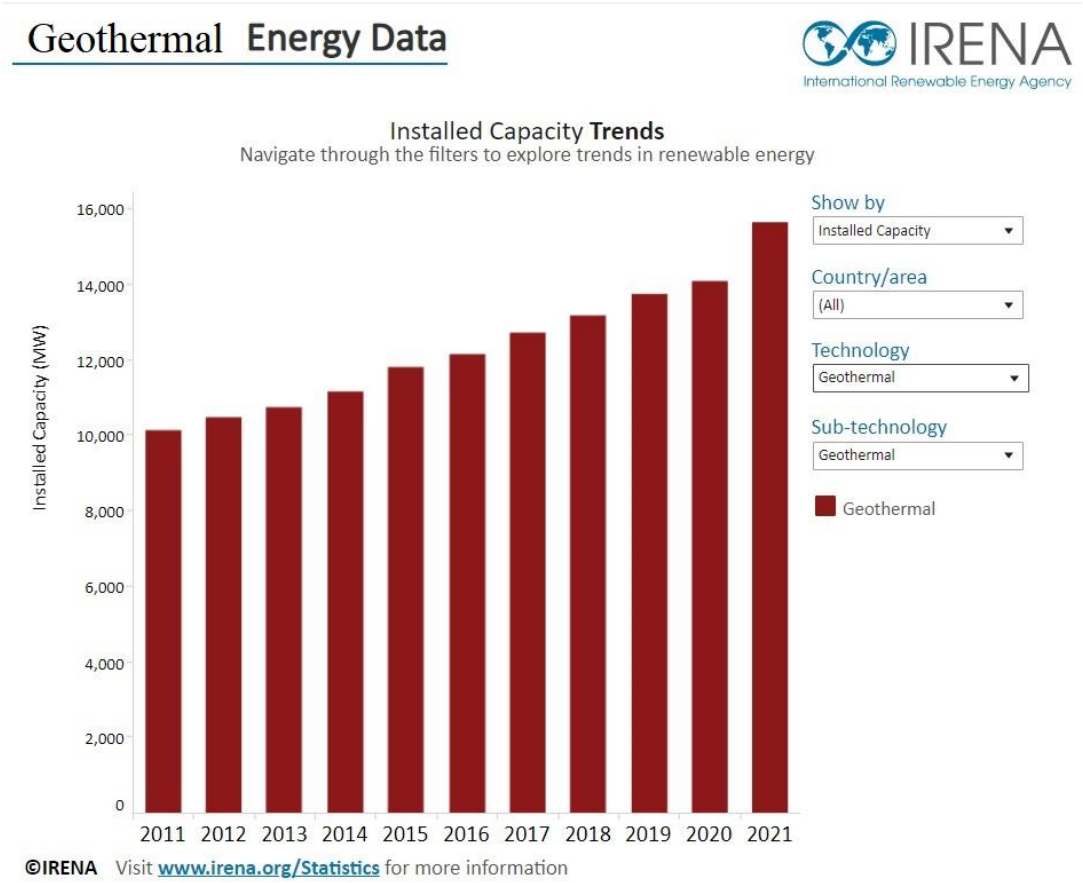

Figure A2.7. Global geothermal energy installed capacity trends (From IRENA)

Ocean:

Tidal and wave energy are still in a growth process, but the moon's gravitational pull will always be dominant in the ocean, making it attractive to harness such power. Tidal barrages (several tidal energy methods) , which work like a dam and are positioned in an ocean bay or lagoon, may harm wildlife as it functions similarly to dams. Like tidal power, wave power is generated using structures or devices anchored to the ocean floor on or just below the water's surface. World marine energy installed capacity trends can be seen in Figure A2.5.

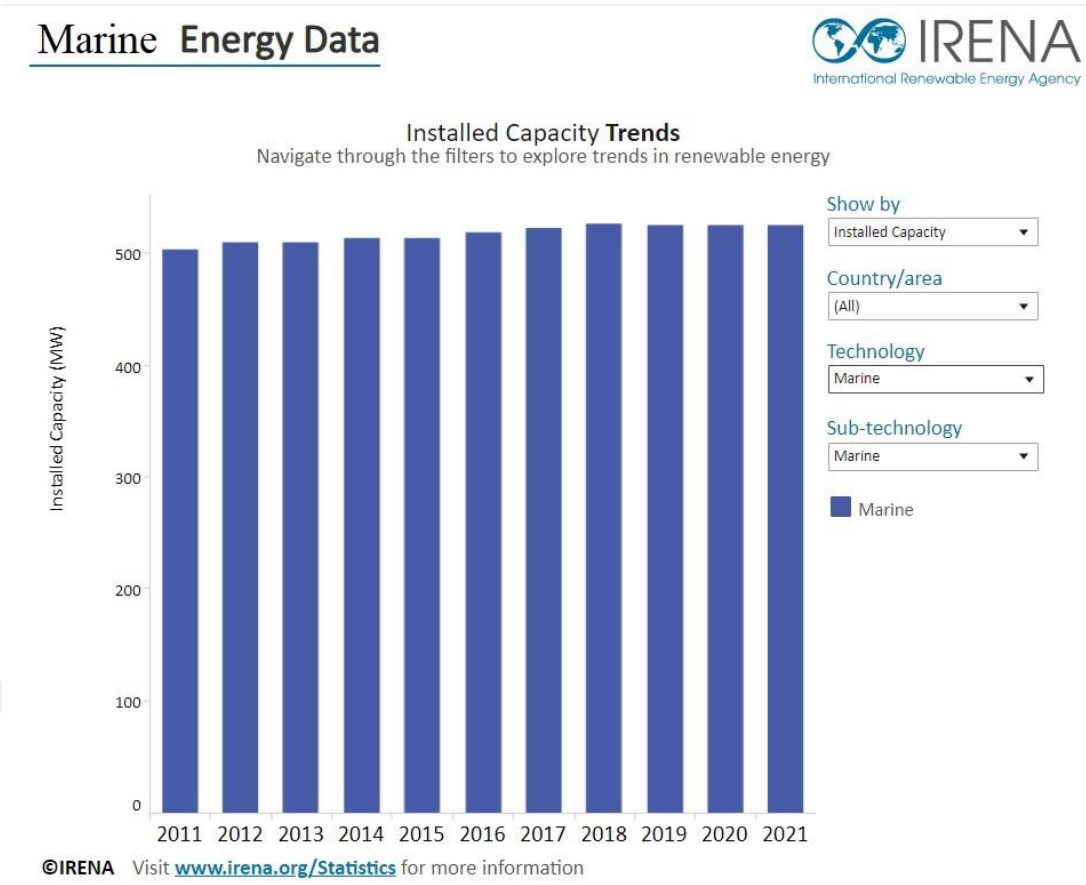

Figure A2.8. Global marine energy installed capacity trends (From IRENA)